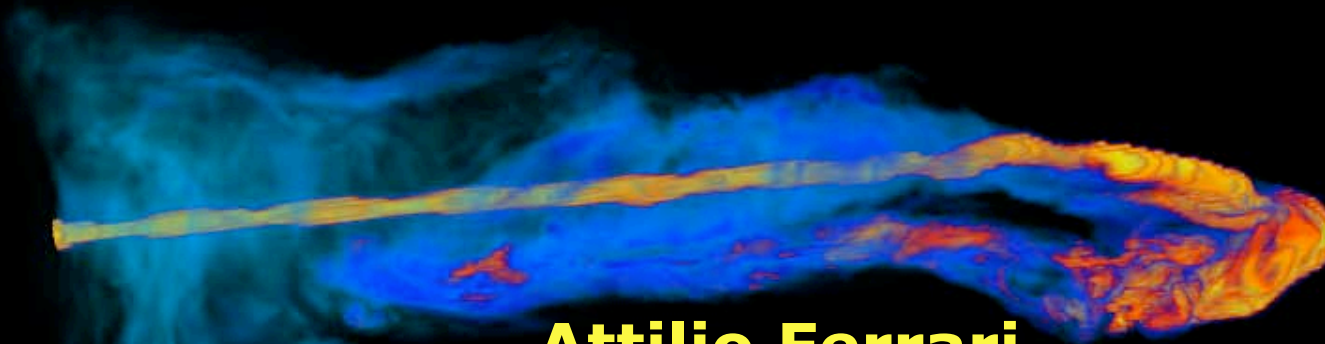


RELATIVISTIC JETS FROM BLACK HOLES



Attilio Ferrari

CIFS Consorzio Interuniversitario per la Fisica Spaziale
Dipartimento di Fisica, Università di Torino
INAF Osservatorio Astronomico di Torino
INFN, Sezione di Torino



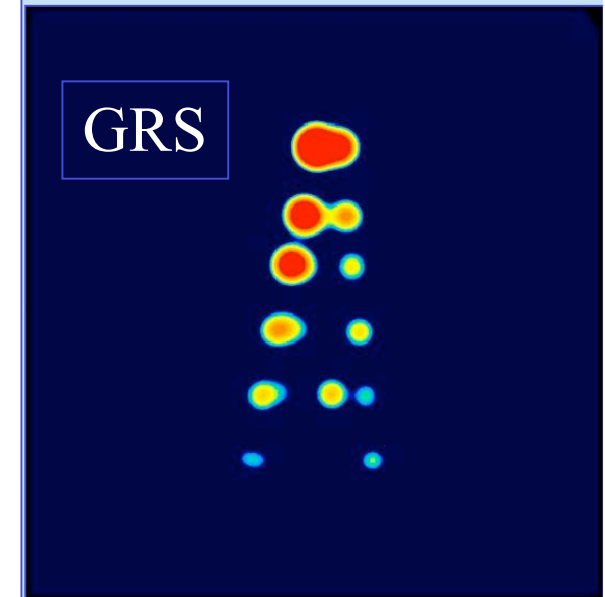
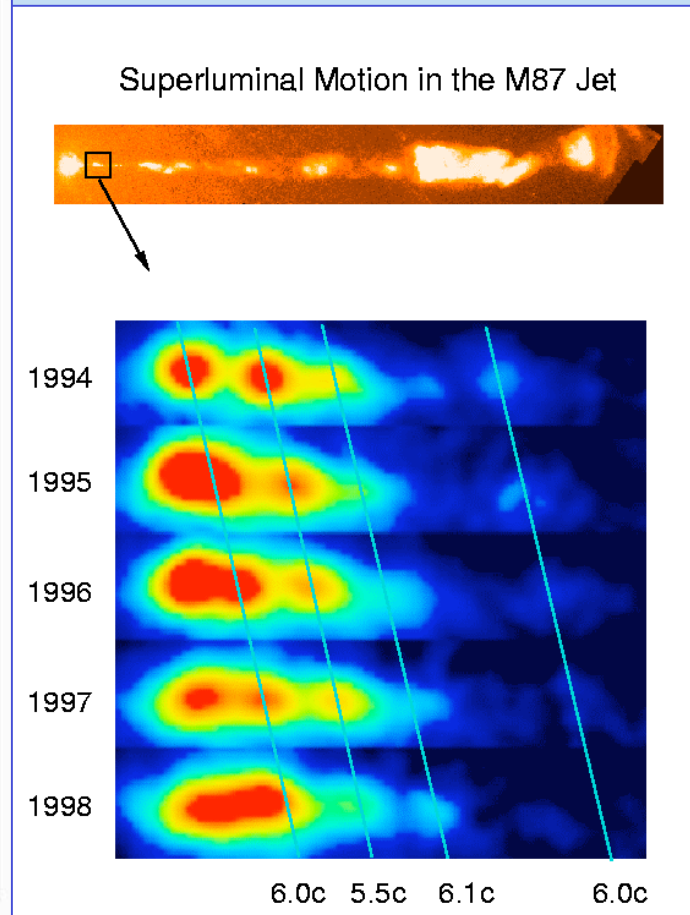
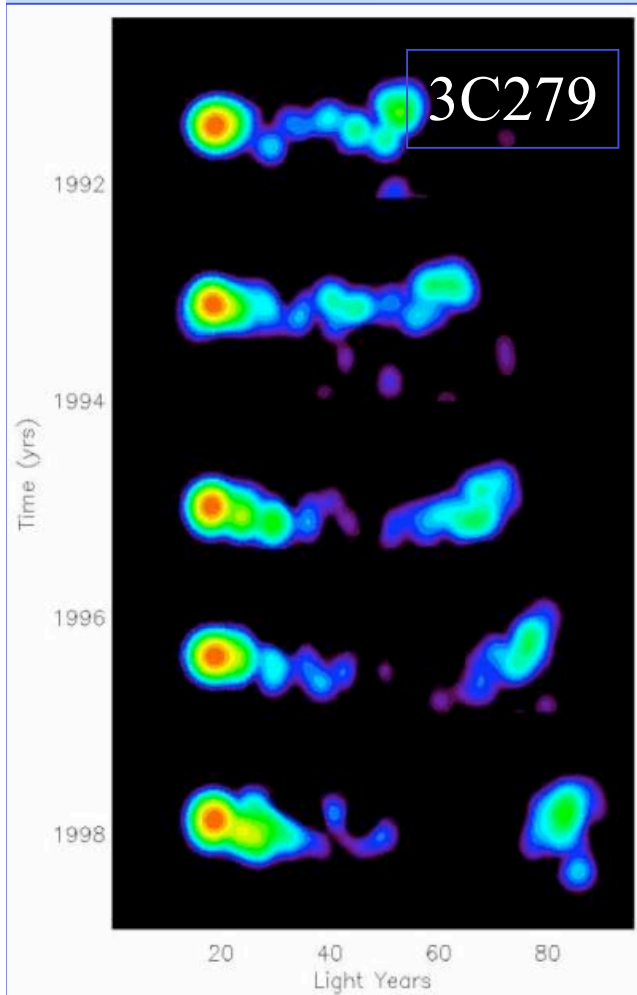
BLACK HOLES IN MATHEMATICS AND PHYSICS
Dubna, 16-17 December 2011



Summary

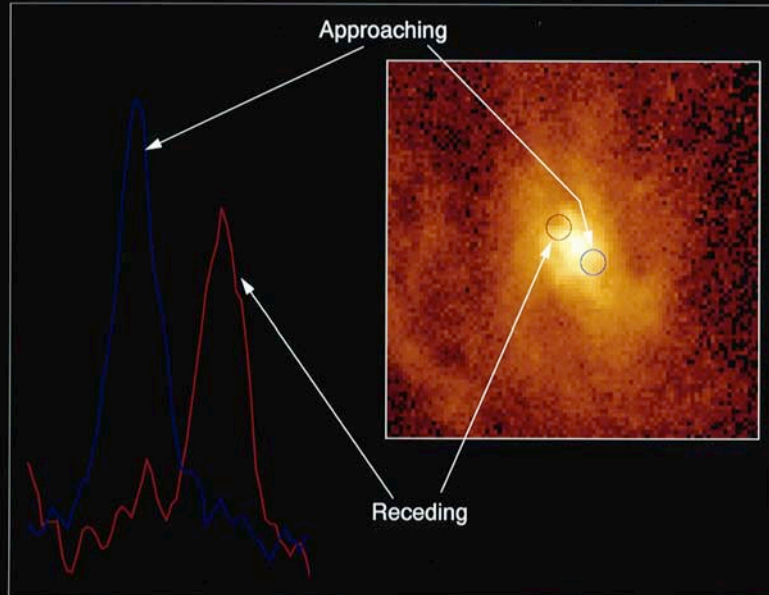
- Jets - BHs astrophysical connection
- Jet launching
- Accretion structure
- Jet propagation
- Simulation validation

Astrophysical Evidence of Relativistic Jets



Superluminal motions & Doppler boosting jet/counter-jet
(Cohen et al. 1971, Biretta et al. 1999, Mirabel et al 1992)

Spectrum of Gas Disk in Active Galaxy M87

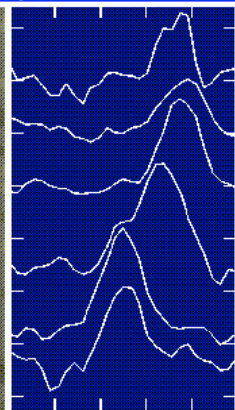
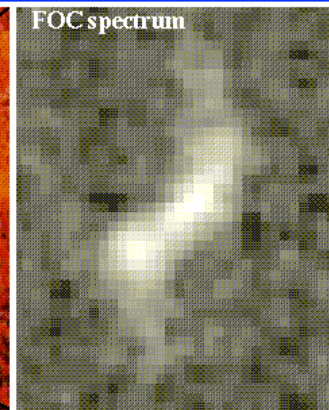
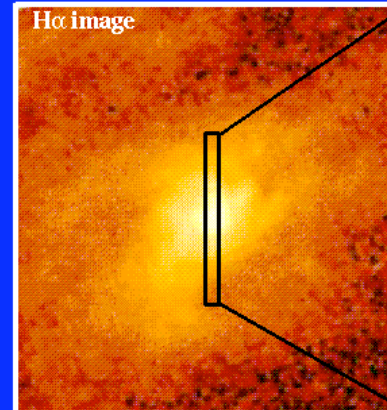
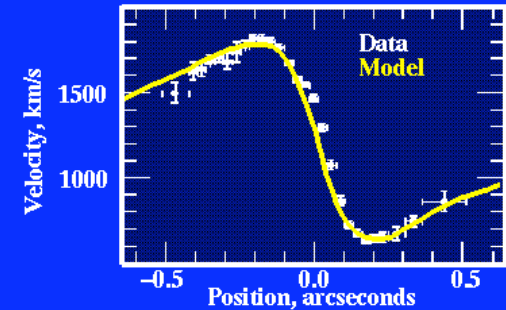


Hubble Space Telescope · Faint Object Spectrograph

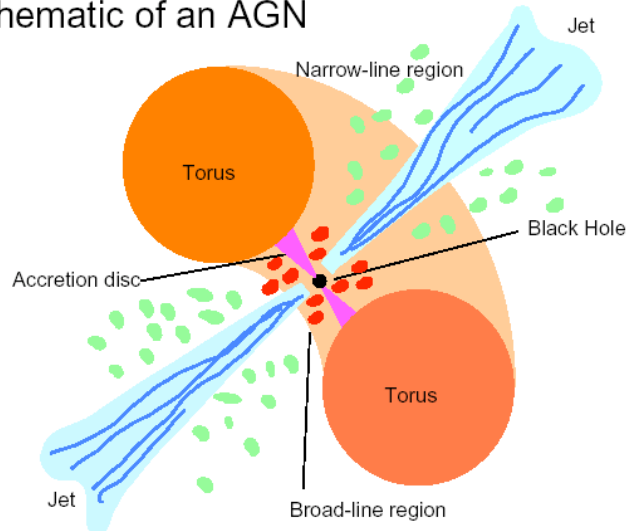
The accretion-outflow paradigm

Velocity Profiles in the M87 Core

Model: central mass 3.2×10^9 solar masses



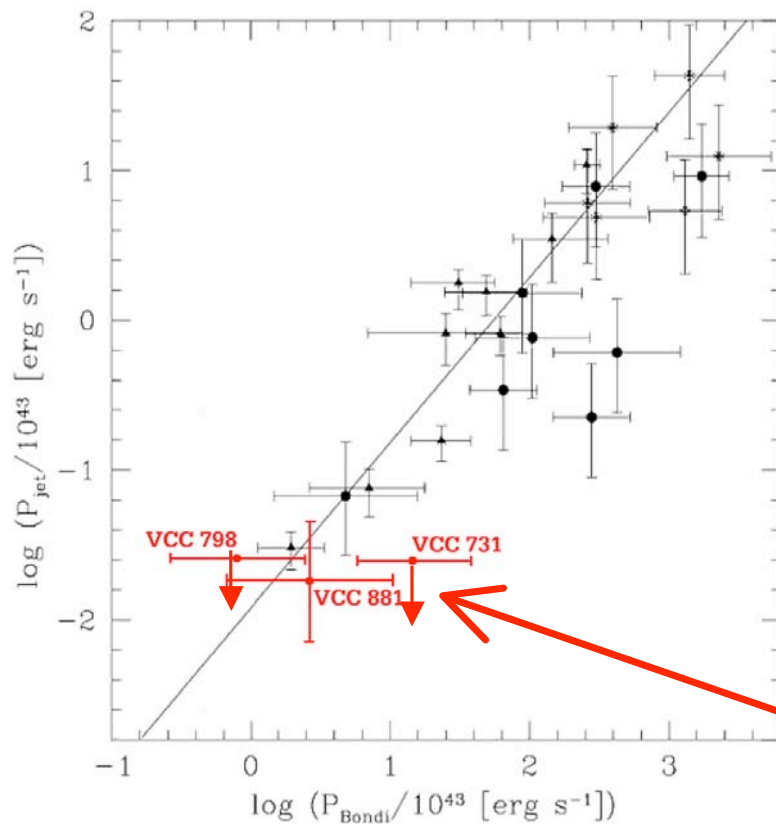
Schematic of an AGN



High resolution photometry and spectroscopy from HST
Compact rotating SMBH

BH accretion and jets

Correlation between accretion onto BH and jet's kinetic power (Allen et al. 2006, Heinz et al. 2007, Balmaverde et al. 2008)

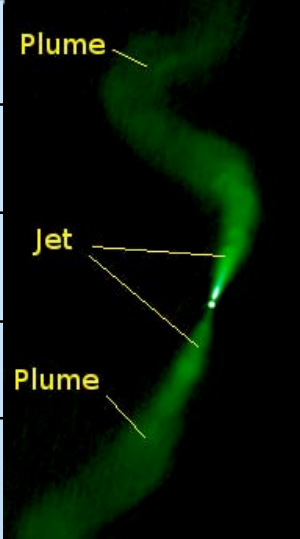
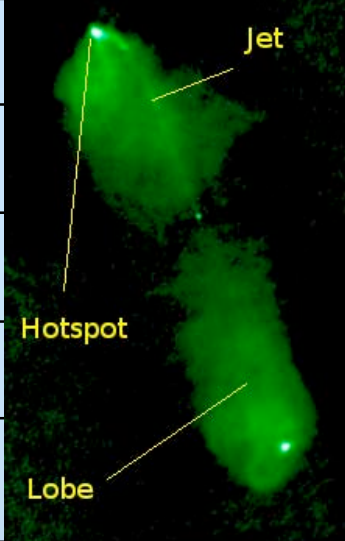
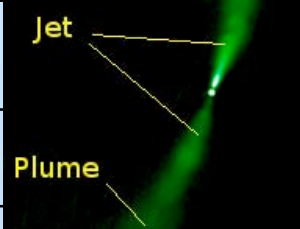
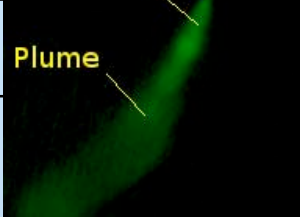


$$1) P_B = \dot{M}_B c^2, \quad \dot{M}_B = \frac{\pi G^2 \rho_B M_{BH}^2}{c_s^3}$$

$$2) P_j = 8.6 \times 10^{22} L_{\nu, \text{radio core}}^{12/17} \text{ erg s}^{-1}, \alpha_\nu = 0$$

Radio quiet

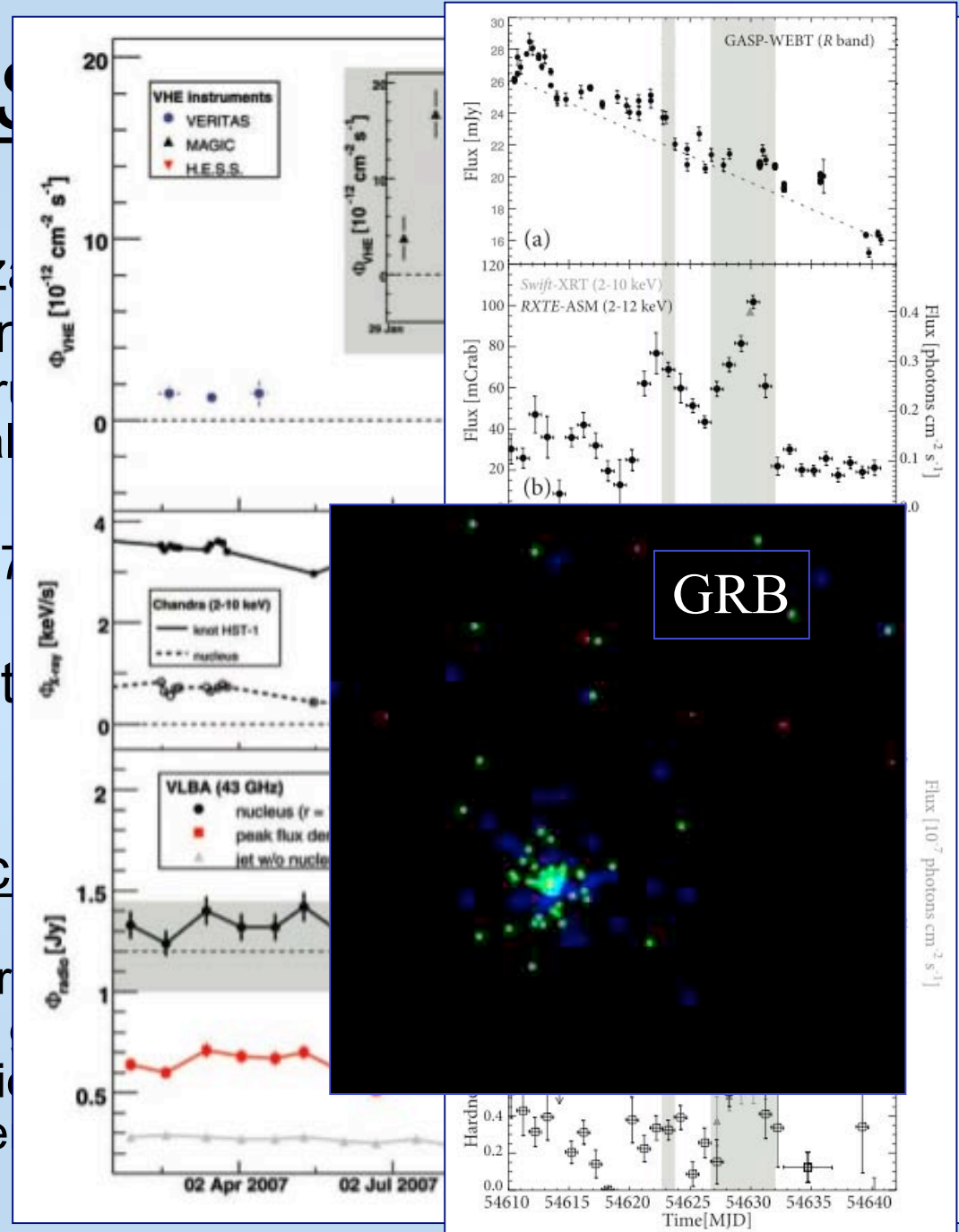
Relativistic radio jets

		FR I	FR II
0.1 pc	$\gamma \approx 10-20$		
1 pc	$\gamma \approx 3-20$		
100 pc	$\gamma \approx 5$		
1 kpc	$\gamma \approx 2$		$\gamma > 10$
10 kpc	$\gamma \approx .2$		$\gamma > 4$

(Giovannini et al. 2005, Laing et al. 2008)

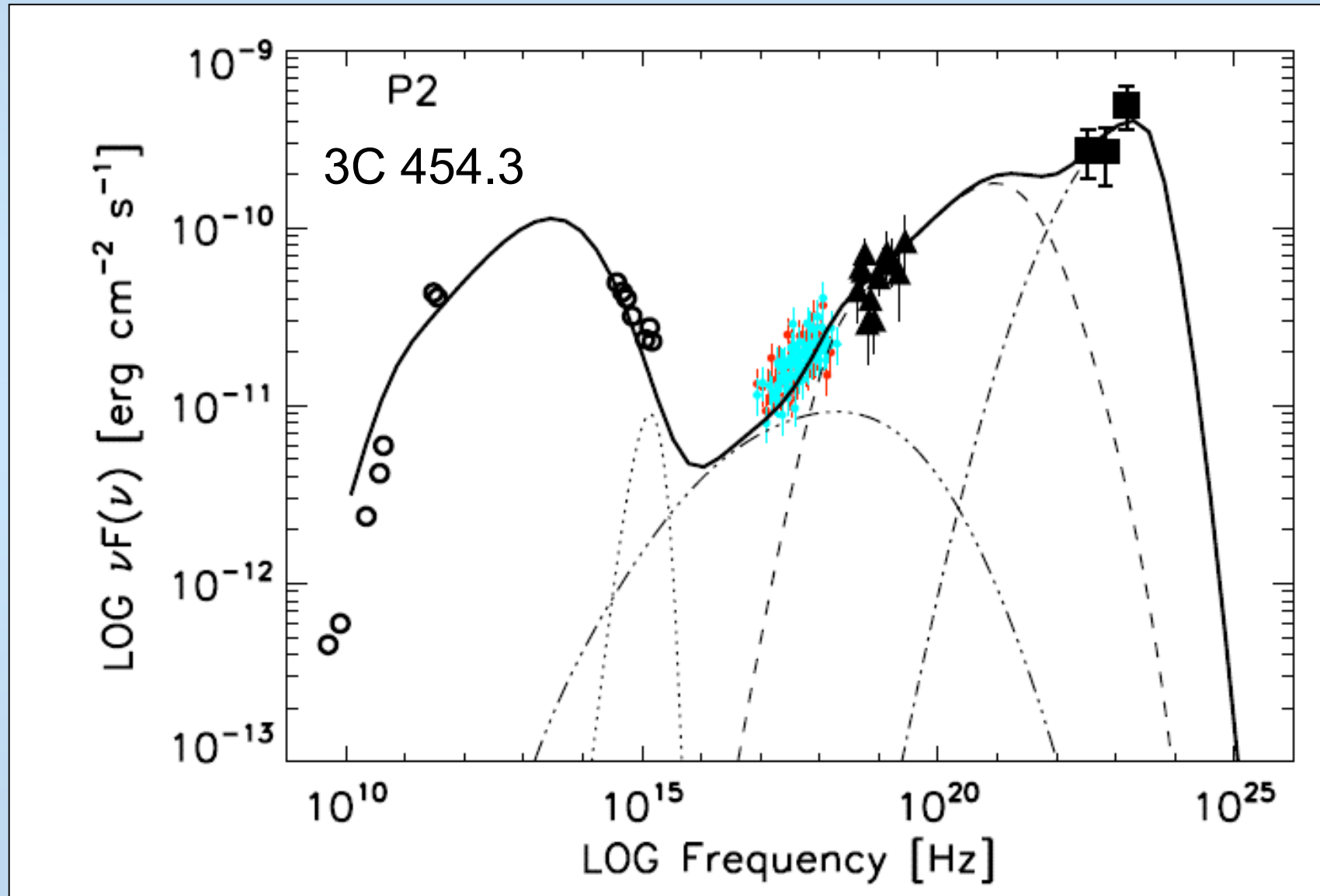
Jets and VHE S

- VHE emission from blazars correlated with X rays and radio
 - Mkn 421 (AGILE, Donnarumma et al. 2007)
 - M87 (FERMI, Acciari et al. 2006)
- GRBs (Klebesadel et al. 1979)
- Doppler boosting in relativistic jets
- Light jets with relativistic speeds
 - Spine produces synchrotron emission, boosted to GeV and TeV
 - Sheath produces radio emission (e.g. Tavecchio et al. 1998)
 - Radio emission from extended jet



HIGH-ENERGY SPECTRA

AGILE 2007

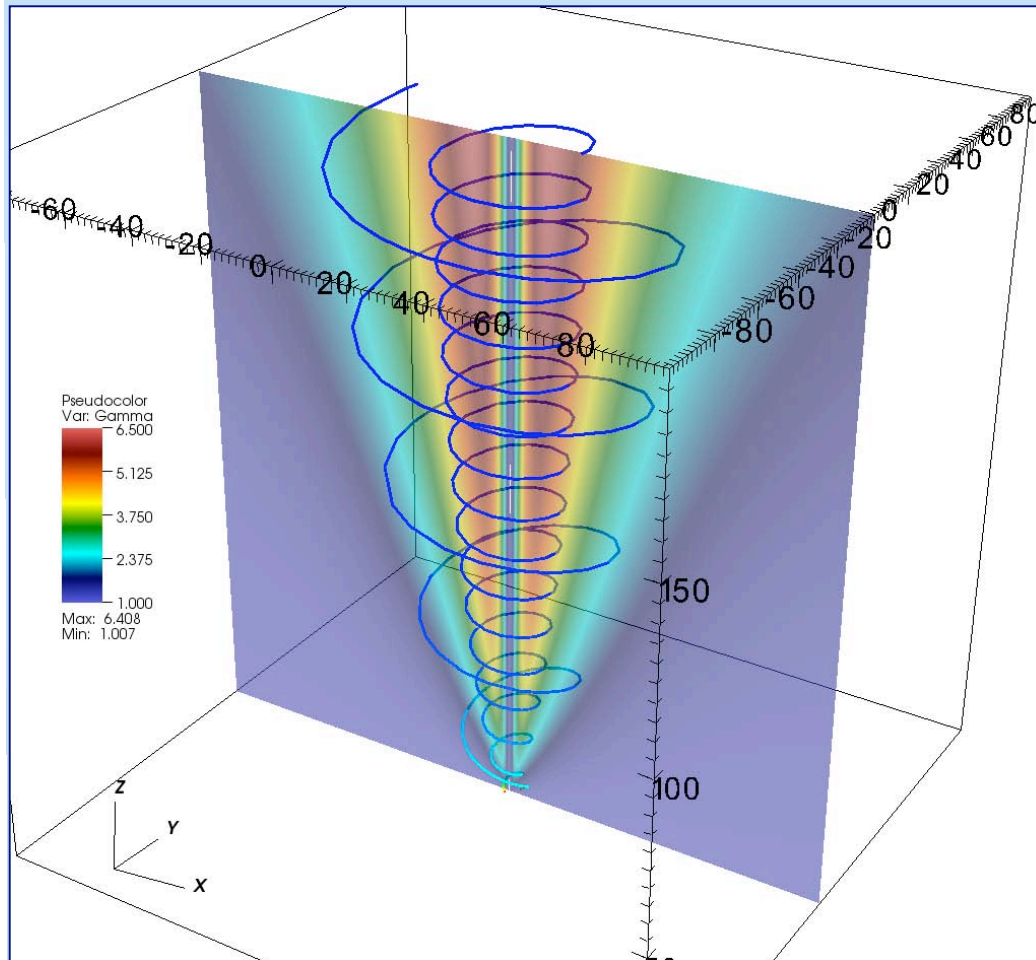


Jet Launching

- Two energy reservoirs:

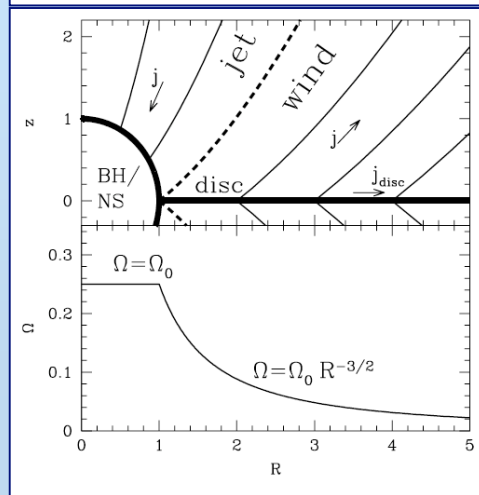
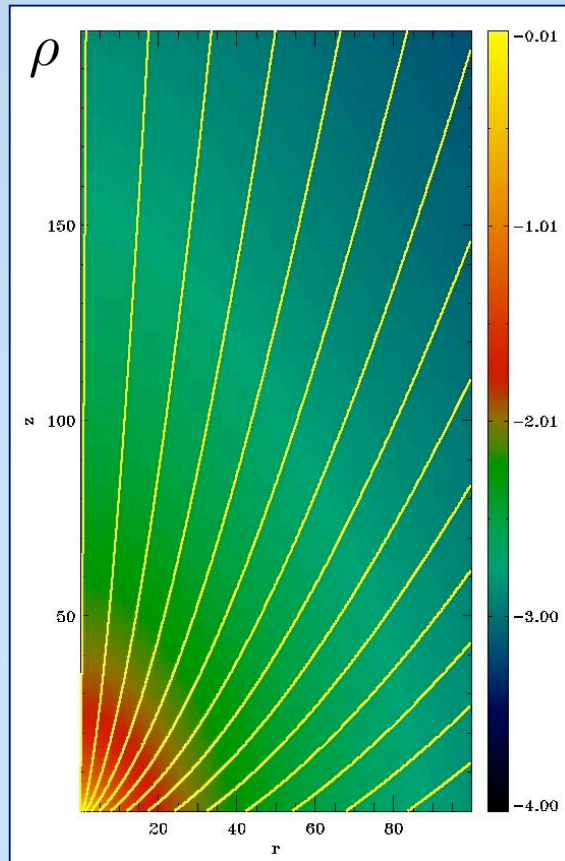
Accretion (e.g. Keplerian disk $\Omega = \Omega_{\text{Keplerian}}$)

Kerr black hole rapid rotation ($\Omega_H = ac/2R_H$ $J_H = aGM^2/c$ $-1 < a < 1$)



- Magneto-centrifugal mechanism
- Resort to twisted magnetic field to extract rotational energy \dot{E} at a rate mainly in the form of Poynting flux
- Mass outflow rate \dot{M}
- The specific energy $\mu = \dot{E}/\dot{M}c^2$ is the maximum possible Lorentz factor of the outflow
- Which is the asymptotic Lorentz factor γ_∞ and the acceleration efficiency ?

Numerical Simulations

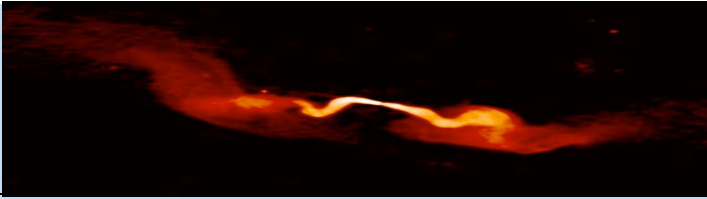


- Highly nonlinear problem
- Special relativistic MHD: focus on large scale acceleration
- Initial and boundary conditions:
 - rotating boundary
[solid rotator (BH/NS) + Keplerian disk]
 - purely poloidal current-free magnetic field
 $B_p \propto r^{-5/4}$ (Blandford & Payne 1982)
 - plasma injected with poloidal speed $\gamma_{inj} \simeq 1$
- Simulation evolved up to stationary state
- Steady state: RMHD axisymmetric invariants

Specific energy: $\mu = \gamma - \frac{r\Omega B_\phi}{\Psi} = \text{kinetic} + \text{Poynting}$



Acceleration = transfer of Poynting to kinetic flux



MHD equations

Non ideal regime inside the disk:
viscous-resistive with radiative losses

$$\frac{\partial \rho}{\partial t} + \nabla \cdot (\rho \mathbf{u}) = 0$$

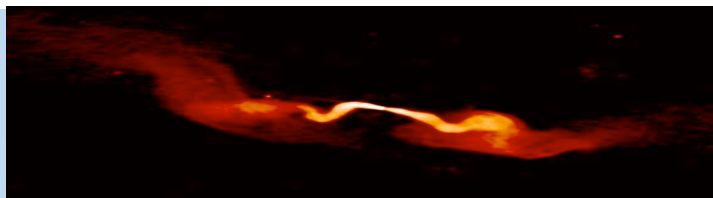
$$\frac{\partial(\rho \mathbf{u})}{\partial t} + \nabla \cdot \left[\rho \mathbf{u} \mathbf{u} + \left(P + \frac{\mathbf{B} \cdot \mathbf{B}}{2} \right) \mathbf{I} - \mathbf{B} \mathbf{B} - \Pi \right] + \rho \nabla \Phi_g = 0$$

$$\frac{\partial e}{\partial t} + \nabla \cdot \left[\left(e + P + \frac{\mathbf{B} \cdot \mathbf{B}}{2} \right) \mathbf{u} - (\mathbf{u} \cdot \mathbf{B}) \mathbf{B} + (\eta_m \mathbf{J}) \times \mathbf{B} \right] - \nabla \cdot (\mathbf{u} \cdot \Pi) = -\Lambda_{cool}$$

$$e = \frac{P}{\gamma - 1} + \frac{\rho \mathbf{u} \cdot \mathbf{u}}{2} + \frac{\mathbf{B} \cdot \mathbf{B}}{2} + \rho \Phi_g$$

$$(\Pi)_{ij} = 2 \frac{\eta}{h_i h_j} \left(\frac{v_{i;j} + v_{j;i}}{2} \right) + \left(\eta_b - \frac{2}{3} \eta \right) \nabla \cdot \mathbf{v} \delta_{ij}$$

$$\frac{\partial \mathbf{B}}{\partial t} + \nabla \times \mathbf{E} = 0 \quad \left(\mathbf{E} = -\mathbf{u} \times \mathbf{B} + \eta_m \mathbf{J}, \quad \nabla \cdot \mathbf{B} = 0 \right)$$



- Consistent treatment of disk-jet system → include the disk in the computational box

How? Solve numerically for equilibrium in r and z , exploit symmetries

Model the disk's "turbulence" →

"alpha" prescription of transport coefficients (Shakura & Sunyaev 1973)

How? $\alpha_m = \frac{\nu_m}{V_A h} \Big|_{z=0}$ $\alpha_v = \frac{\nu_v}{C_s h} \Big|_{z=0}$ $\mathcal{P}_m = \frac{\nu_v}{\nu_m} \Big|_{z=0}$ *Only inside the disk* $\exp\left(-2\frac{z^2}{H^2}\right)$

- Launching via magneto-centrifugal mechanism → large scale magnetic field

How? $\Psi = \frac{4}{3} B_{z0} r_0^2 \left(\frac{r}{r_0}\right)^{3/4} \frac{m^{5/4}}{(m^2 + z^2/r^2)^{5/8}}$ $B_z = \frac{1}{r} \frac{\partial \Psi}{\partial r}$ $B_r = -\frac{1}{r} \frac{\partial \Psi}{\partial z}$

- "Warm" outflows → allow for entropy generation inside the disc

How? $\Lambda_{cool} = f_m Q_{Ohm} + f_u Q_{visc}$ $f_m = f_u = 0$ → "warm" $f_m \neq f_u \neq$
 $f_m = f_u = 1$ → "cold"

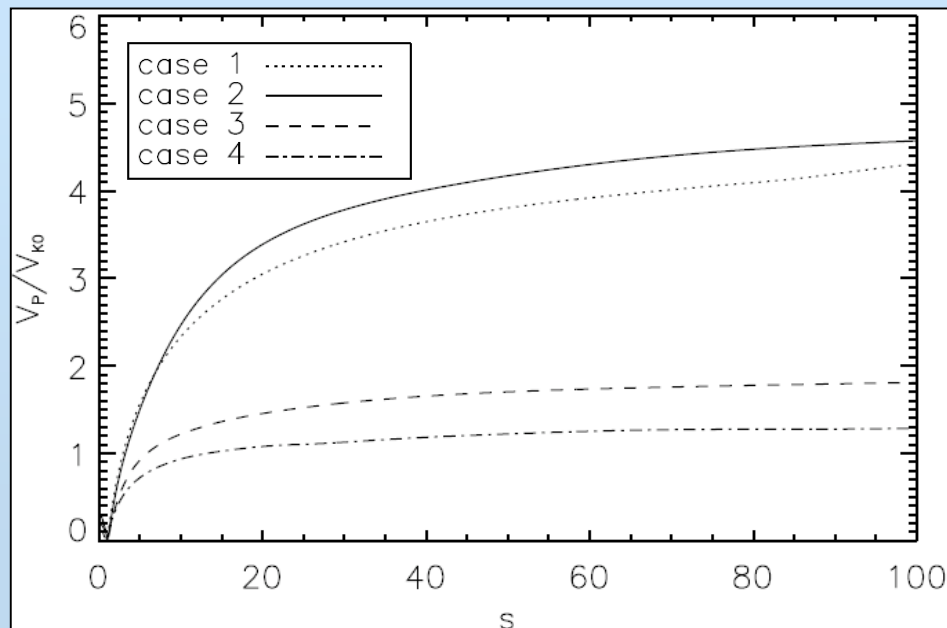
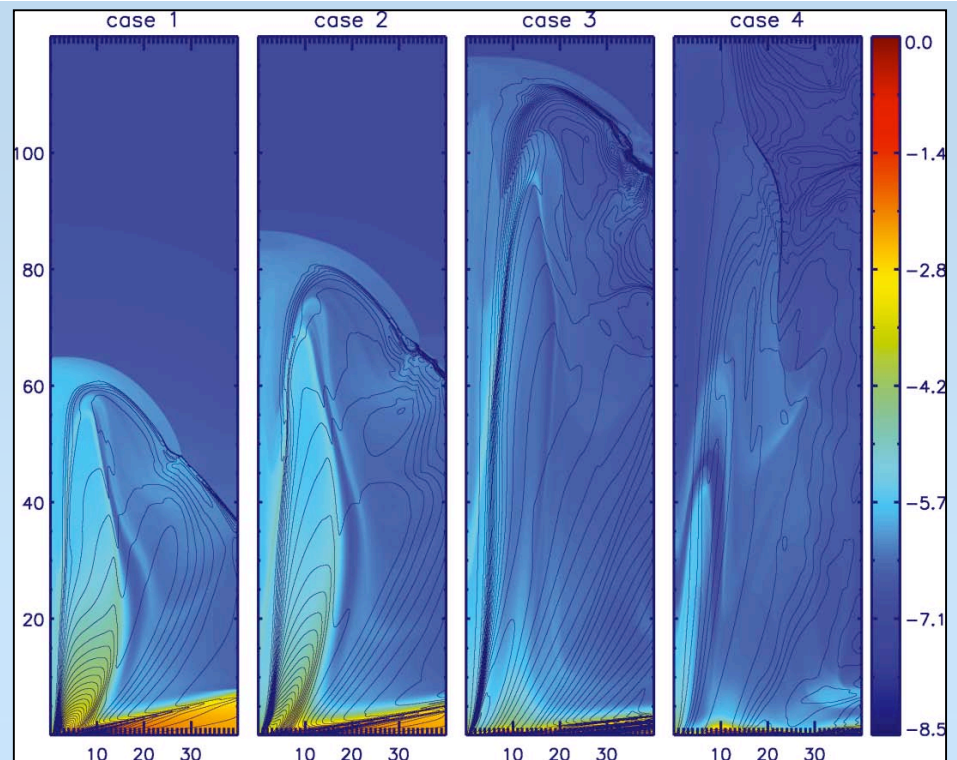
- *Focus: magnetization*
- Resistive 2.5D MHD simulations of jet launching:

$$\mu = 2P / B^2$$

- From weak (case 1, 2) to strong magnetic fields (case 3, 4)

$$1/3 \leq \mu \leq 10.0$$

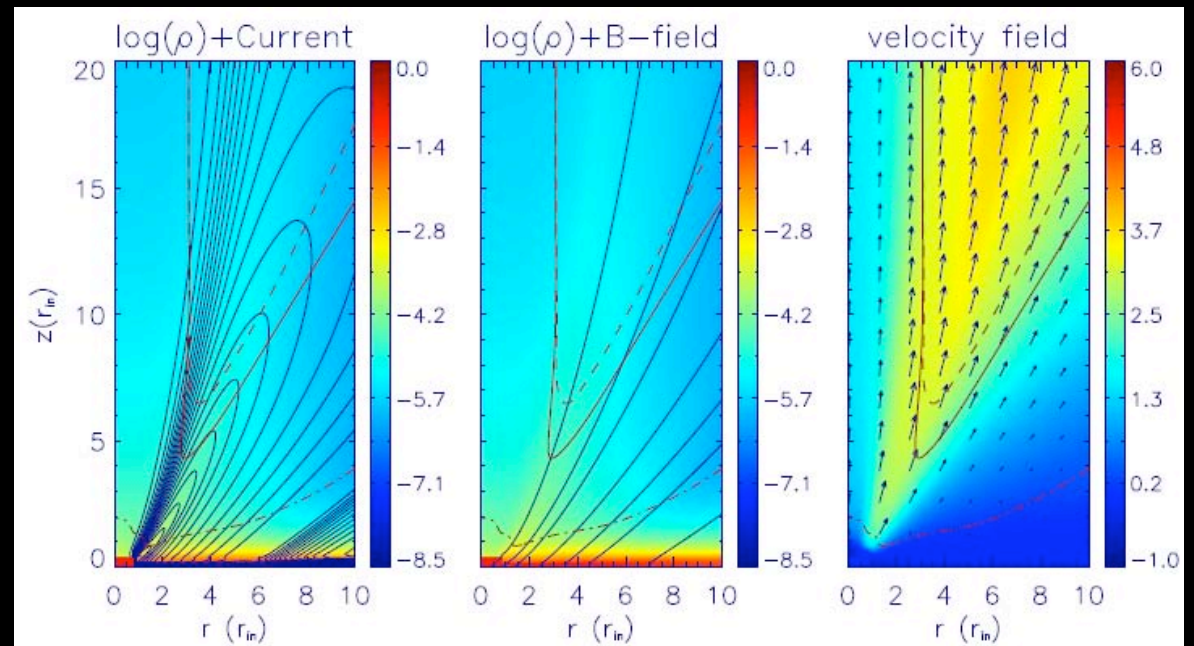
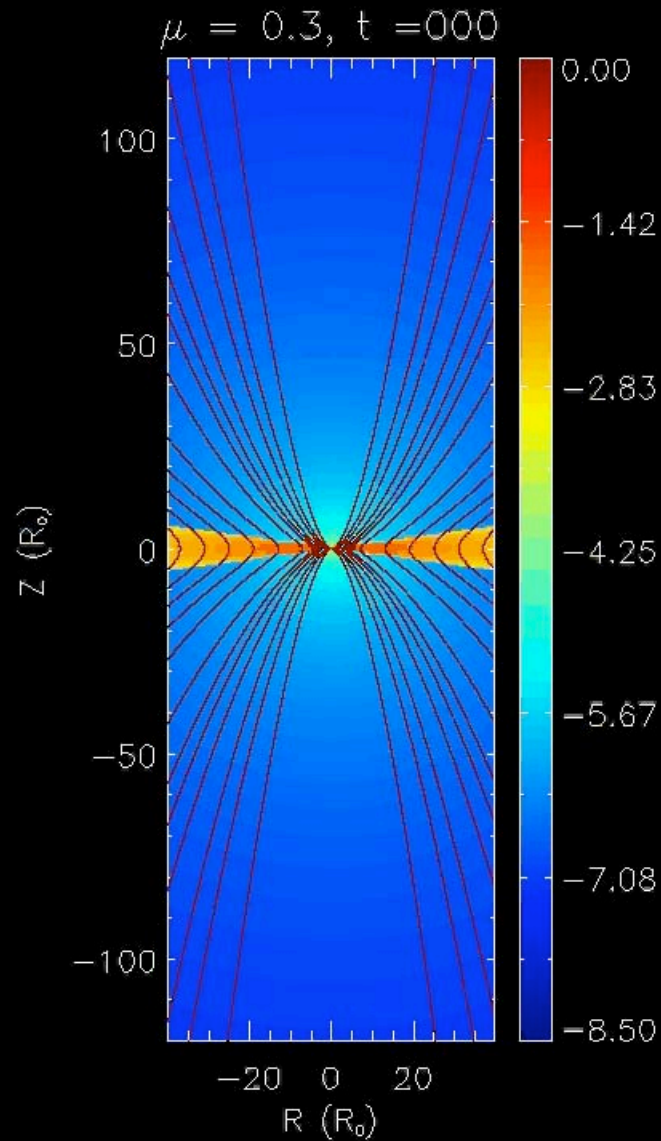
Tzeferacos et al. MNRAS 2009



- Self-consistent jet ejection from accretion disc
- Super Alfvènic, super fast magneto-sonic outflows
- *Steady state solutions obtained only above equipartition plasma μ (case 1,2)*

- Temporal evolution for case 2

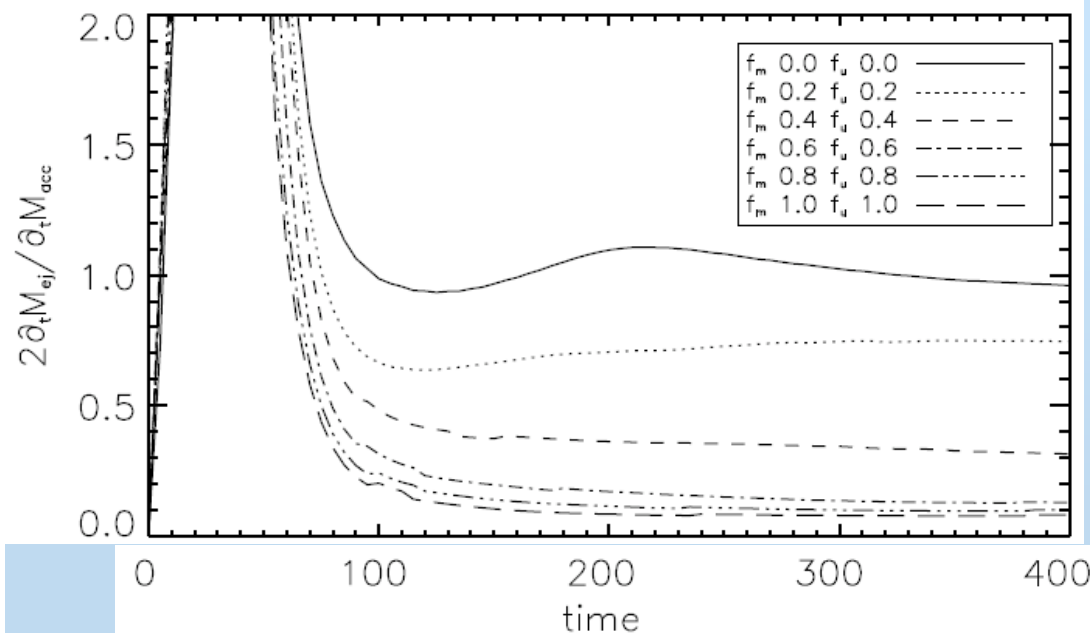
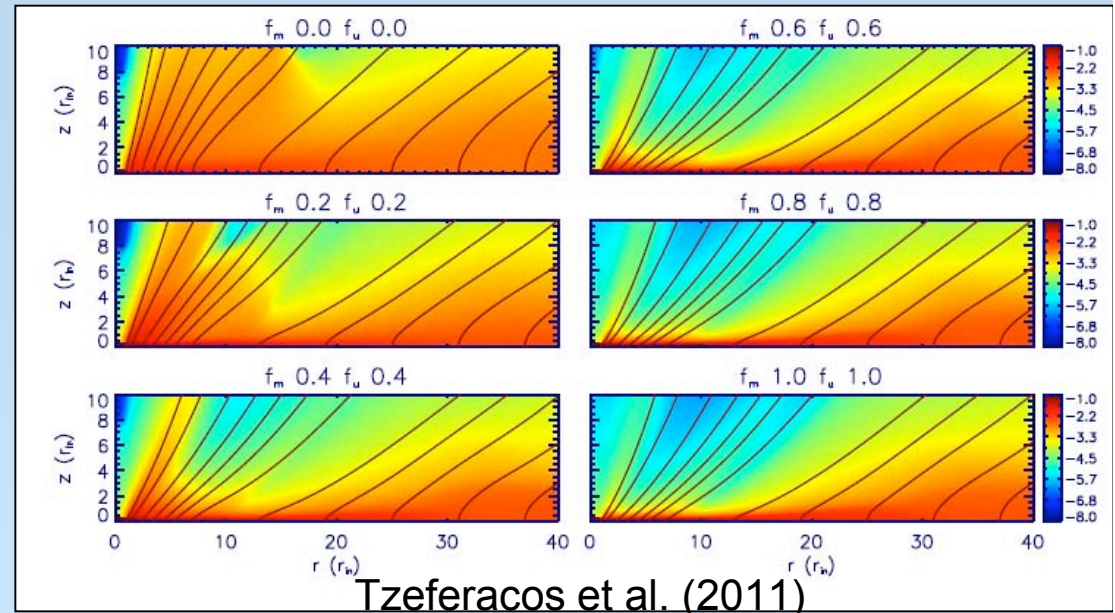
- Close-up on the ejection region



- Focus: entropy generation due to viscous and Ohmic heating

- Viscous and resistive 2.5D MHD simulations of jet launching

- α prescription for viscosity and resistivity, with magnetic Prandtl number: $P_m = \eta_u / \eta_m \sim 1$

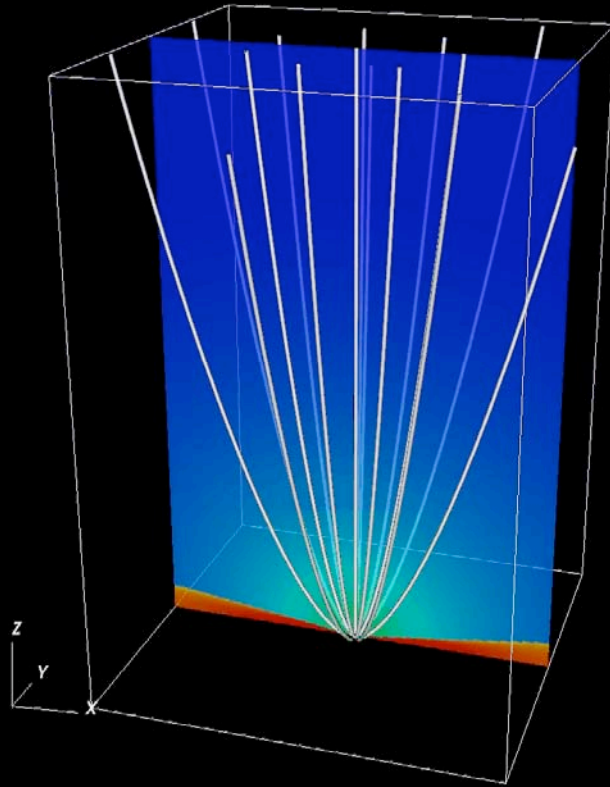


- Strong correlation between disk heating effects and mass loading.

- Efficient acceleration and stationarity is found for mildly warm and cold cases, comparable to slow radio-galaxies and YSO jets

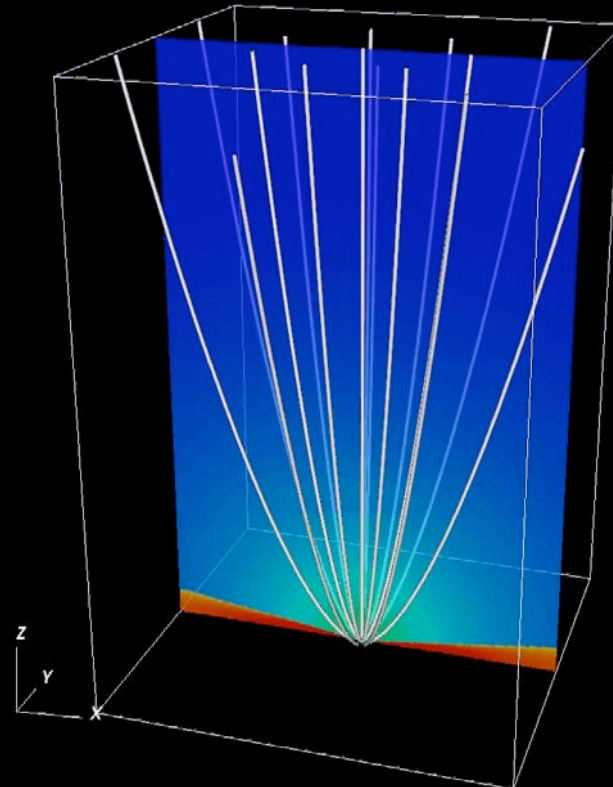
cold

Density (log) + magnetic field lines



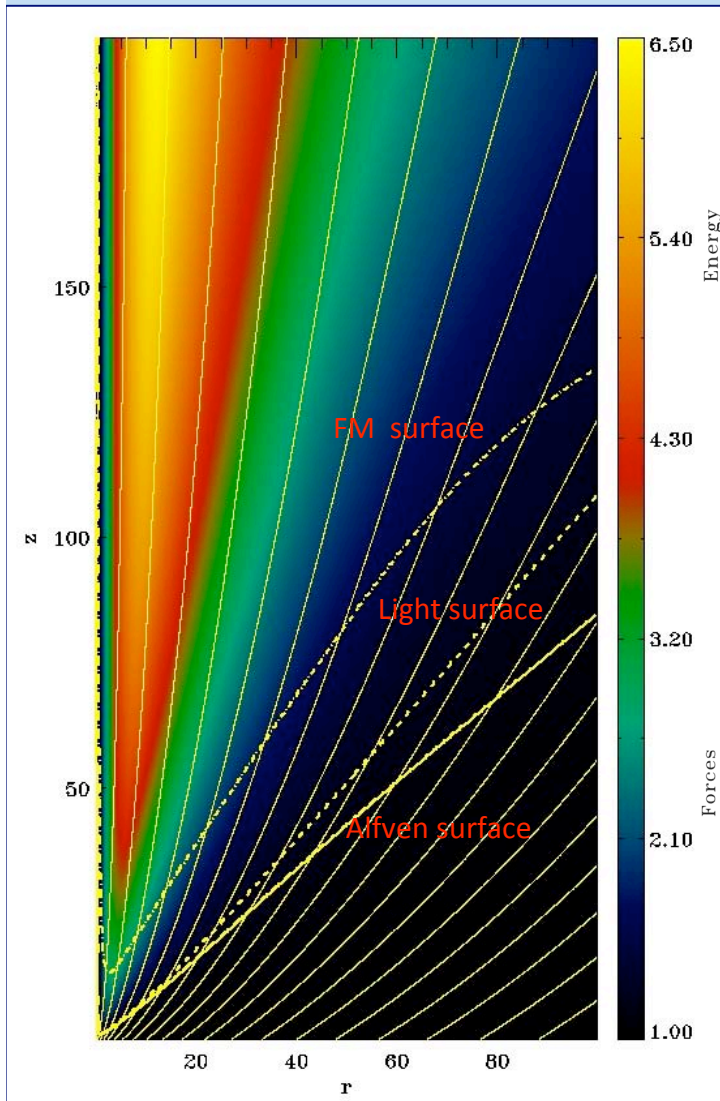
warm

Density (log) + magnetic field lines

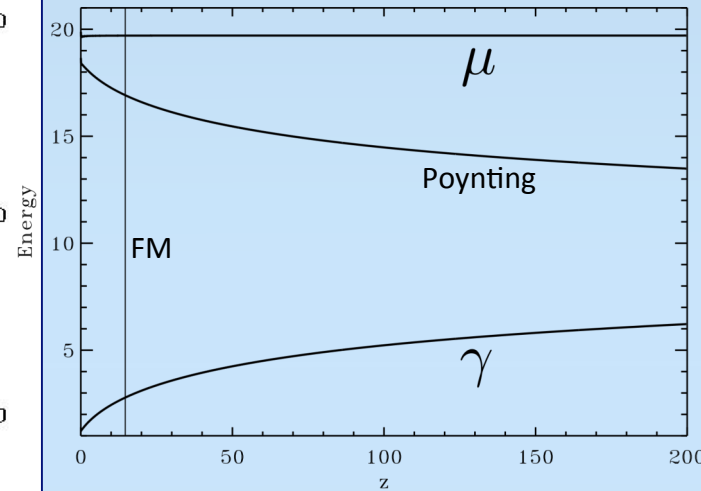


Jet Acceleration

Lorentz Gamma

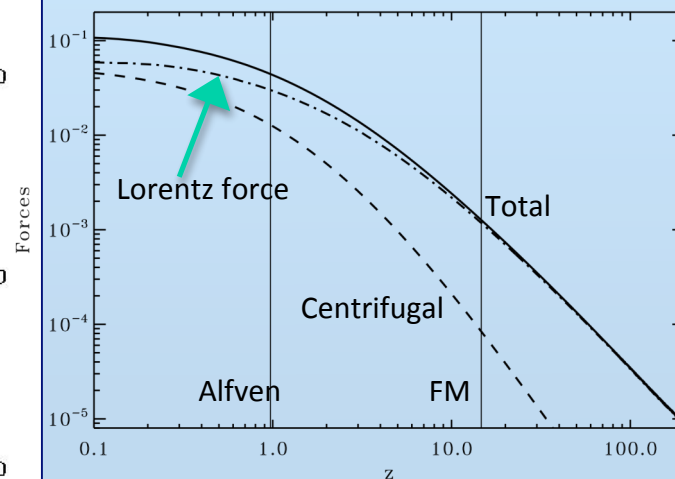


Along a magnetic surface with $r_0 = 1$



- Flow accelerates even beyond FM surface up to $\gamma \sim 6$ with an efficiency $\gamma \sim 0.3\mu$

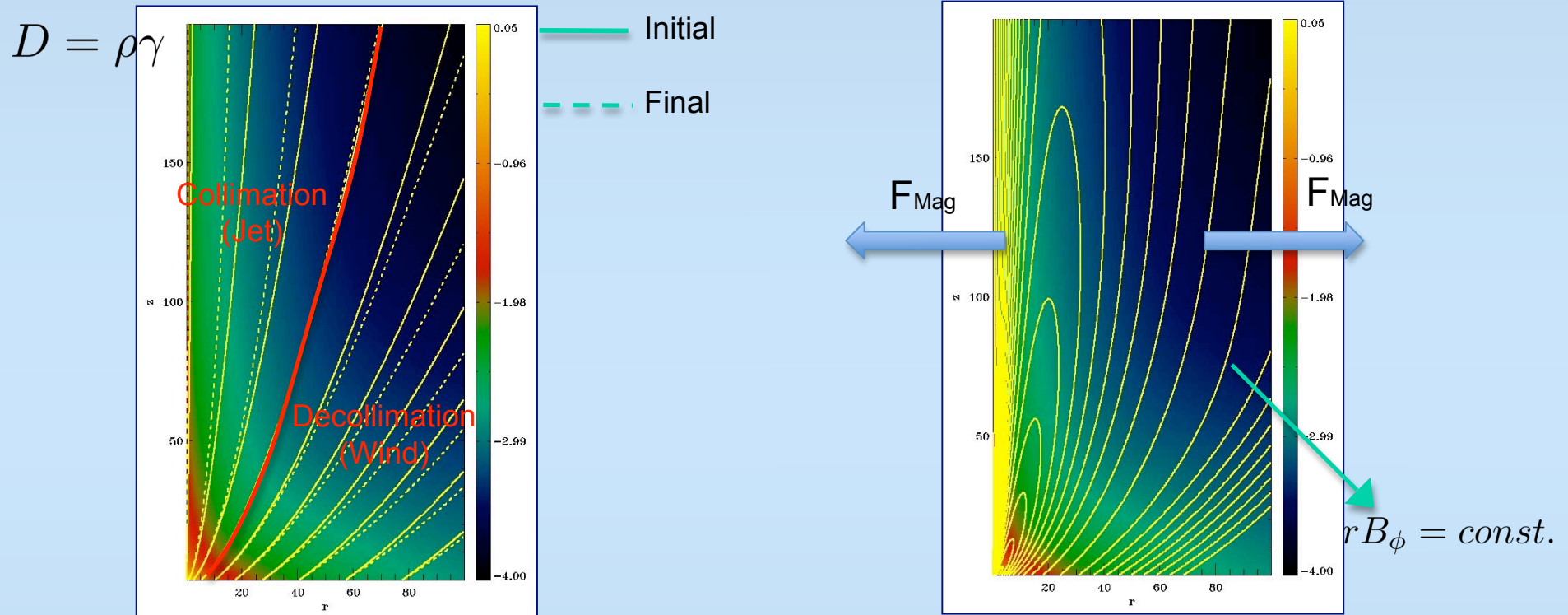
- Flow is still accelerating! (need larger domains)



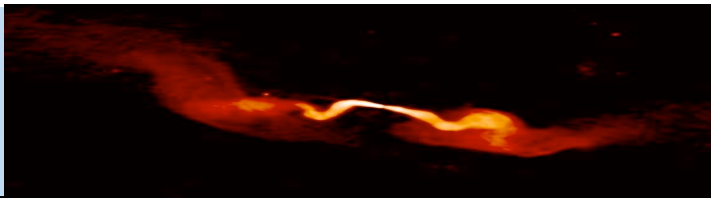
- Flow accelerated by Lorentz forces (B_ϕ pressure) and centrifugal effects

- Beyond FM surface magnetic pressure drives the flow (magnetic nozzle, Li et al. 1992)

Jets, winds and (de)collimation

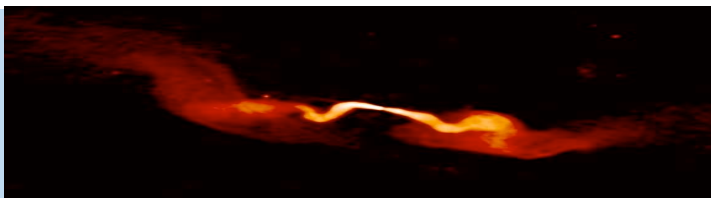


- The magnetic force associated with the toroidal field (perpendicular to the $rB_\phi = const.$ isosurfaces) tends to collimate the inner field lines and to decollimate the outer ones, creating a configuration favorable for efficient acceleration.
- The structure suggests a fast jet (collimated) – slower wind (decollimated) configuration.
- In the relativistic regime, the electric force is comparable to the magnetic but with opposite sign: differential collimation and acceleration are still possible but on very long spatial scales.



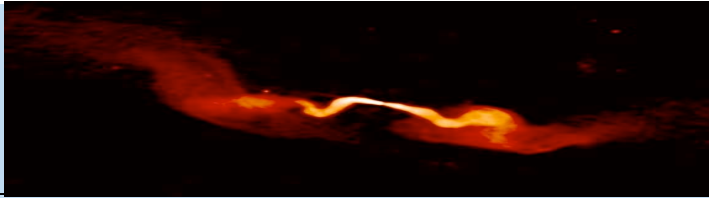
AGN Jet observations

- AGN jets are usually observed at parsec scales (VLBI) while simulations treat milli-parsec scales
- Jets from AGN have usually flow velocities comparable to the speed of light and Lorentz factors larger than unity
- Assuming a BH of $\sim 10^8 M_{\odot}$ the resulting ranges for the flow velocities are $0.39 \leq \beta \leq 0.72$ and $1.09 \leq \gamma \leq 1.44$ for $0.4 \leq \langle f \rangle \leq 1$
- ✓ For the radio galaxy 6251, Sudou et al. (2000) inferred a bulk acceleration from $0.13 c$ to $0.42 c$ in sub-parsec scales, compatible with intermediate warm solutions



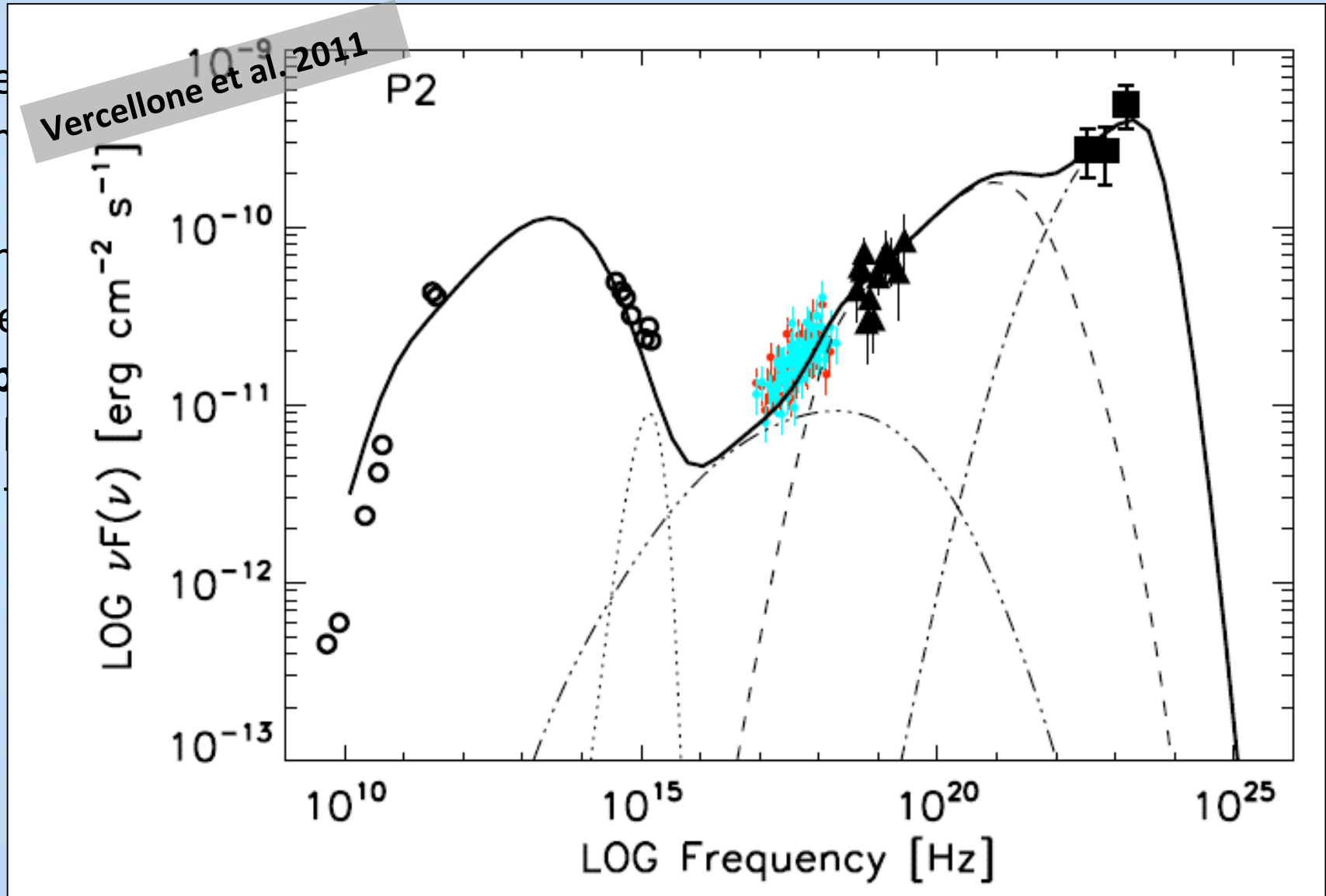
AGN Jet observations

Name IAU	Name other	Type	θ range degree	β range v/c	γ range	Motion β_a
0836+29	4C29.30	FR I	< 35	> 0.55	> 1.20	
1101+38	Mkn 421	BL-Lac	< 30	> 0.87	> 2.03	1.5
1142+20	3C 264	FR I	~ 50	~ 0.98	~ 5.0	
1144+35		FR I	20 - 25	≥ 0.95	≥ 3.2	2.7
1217+29	NGC 4278	LPC	–	–	–	
1222+13	3C 272.1	FR I	60 - 65	$\gtrsim 0.9$	≥ 2.29	
1228+12	3C 274	FR I	< 19	$\gtrsim 0.99$	$\gtrsim 6$	6
1322+36	NGC 5141	FR I	$\lesssim 58$	$\gtrsim 0.54$	$\gtrsim 1.19$	
1441+52	3C 303	FR II	< 40	> 0.7	> 1.4	
1626+39	3C 338	FR I	~ 85	~ 0.8	~ 1.7	0.8 - 0.9
1641+17	3C 346	FR II	< 30	> 0.8	> 1.7	



AGN Jet observations

- ✓ The energy and dynamics
- ✓ Recent discussions of hot plasma by jet emission and/or



Challenging the alpha prescription

Momentum transport
“Viscosity” of α -disks:

$$\nu = \alpha c_s H e^{-2\left(\frac{z}{H}\right)^2}$$

Alpha and disk physical
parameters?

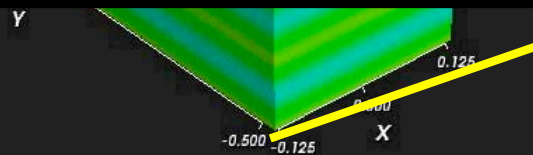
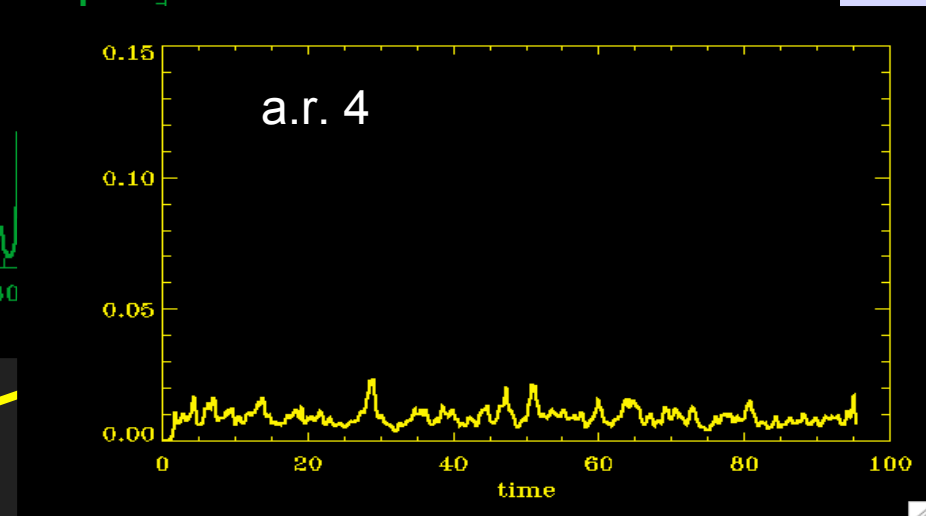
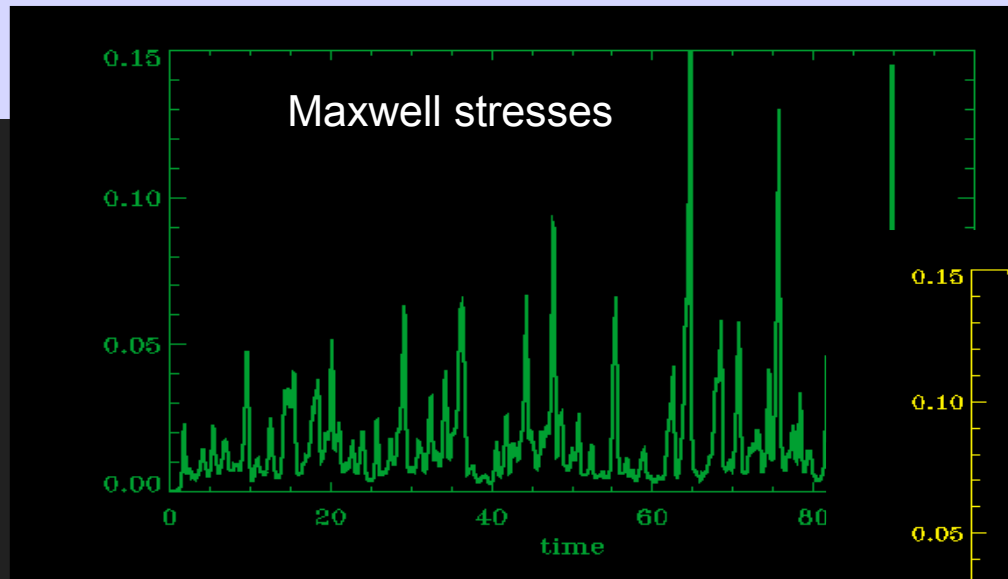
“Measured” values of α

Numerical simulations of MRI <i>varies with large-scale field, dissipation terms</i>	10^{-3} - 10^{-1}
Protostellar disks <i>based on disk masses, temperatures, accretion rates, and lifetimes</i>	10^{-2} - 10^{-3}
Cataclysmic variables <i>based on models of “dwarf nova” outbursts</i>	10^{-3} - 10^0
AGN <i>direct observational constraints are few to none</i>	?

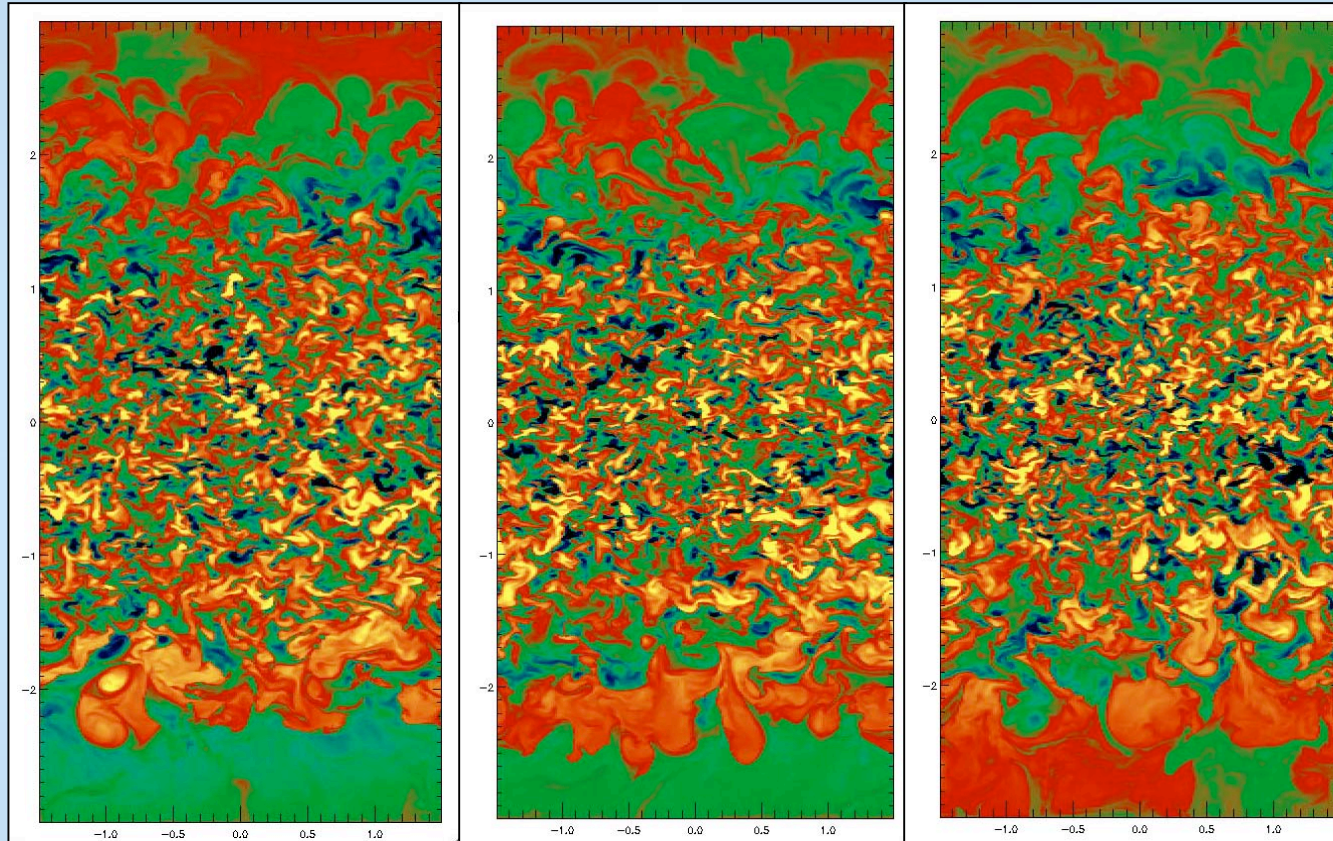
Numerical simulations of Magneto-Rotational Instability
Effects of the numerics?

3D high-resolution simulation
in shearing box approximation
(Sano & Inutsuka 2001, Mignone et al 2009)
In a cartesian frame of reference corotating
with the disk
The channel solution, intermittent states,
transition to turbulence, calculation of
Maxwell stresses, aspect ratio dependence
Dynamo
Maxwell stresses and alpha

Unstratified shearing boxes have been
shown to suffer from many problems
(Fromang et al. 2007, Regev & Umhuran
2008, Bodo et al. 2008, 2010, 2011)
In particular with zero mean
field the transport becomes
negligible at high Reynolds
numbers: artifact of shearing box
Towards global simulations

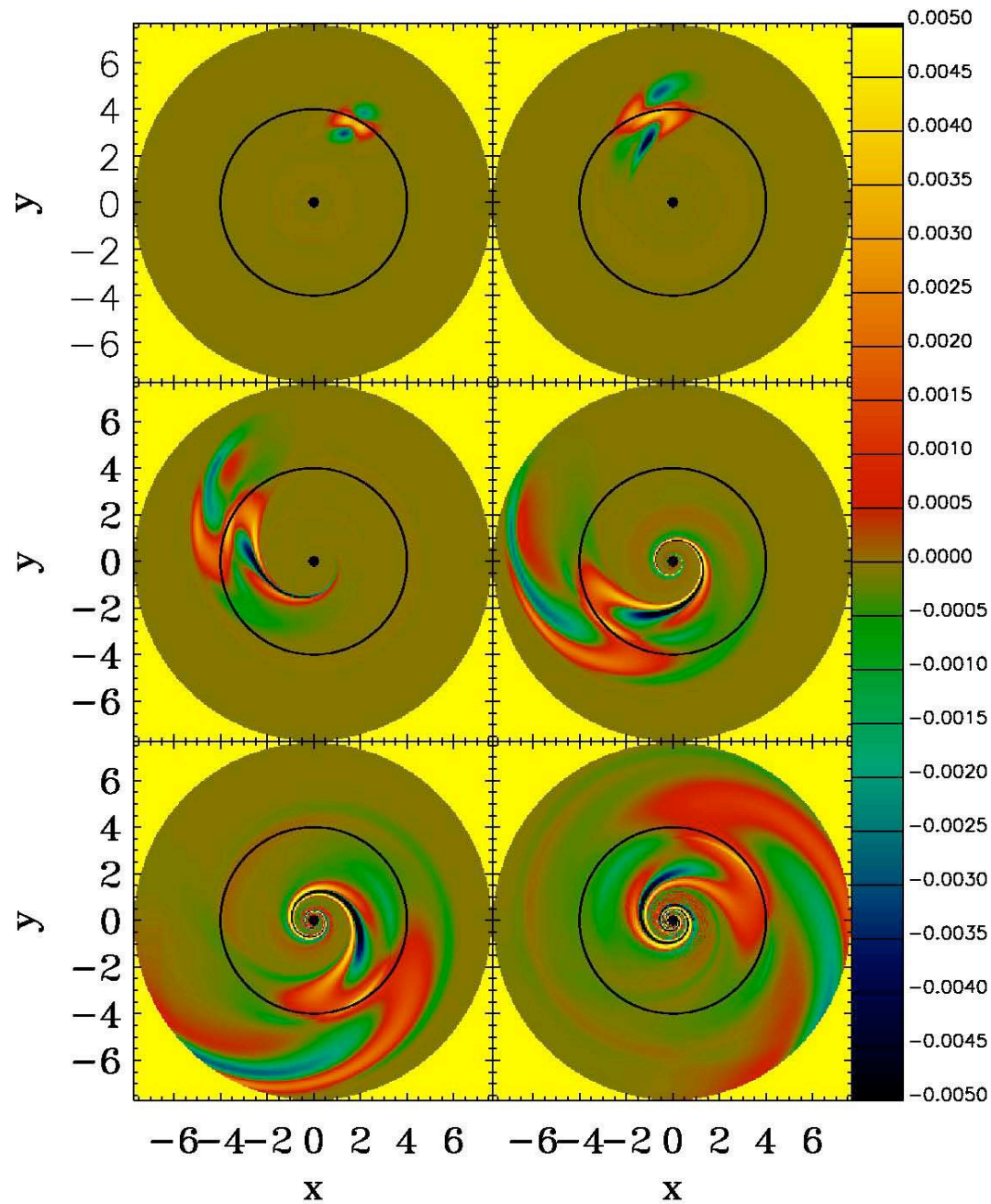


Preliminary results from simulations in which gravitational stratification is included
Still shearing box conditions in the radial direction. First step towards global simulations.



Azimuthal
Component
of the magnetic
field.
x-z cut

Domain size $3H \times 4H \times 6H$ (H density scale height). 200 points per scale height.
Turbulent region in the denser region in the middle
Periodic formation of highly magnetized regions in the upper and lower
regions (magnetized coronae)



Momentum
transport
in Keplerian disks

Vorticity

Global solutions
non-normal mode
analysis

(Bodo et al. 2007)

Relativistic Jet Propagation

- Are jets stable ?
- Do they dissipate magnetic flux ?
- Intrinsic/external instabilities
- How do jets decelerate without decollimating ?
- Mass entrainment from the ambient medium across an unstable boundary layer
 - *“internal”* entrainment: diffusion of mass lost from stars within the jet volume (Komissarov 1994)
 - *“external”* entrainment: ingestion of ambient gas from the surrounding IGM via a turbulent unstable boundary layer (Begelman 1982; De Young 1996)
- Connecting morphologies with dynamics
- Instabilities and turbulent particle acceleration

Magnetized Jets

□ $M =$ Mach Number; $\eta = \rho_{\text{amb}}/\rho_{\text{jet}}$; $\gamma =$ Lorentz factor

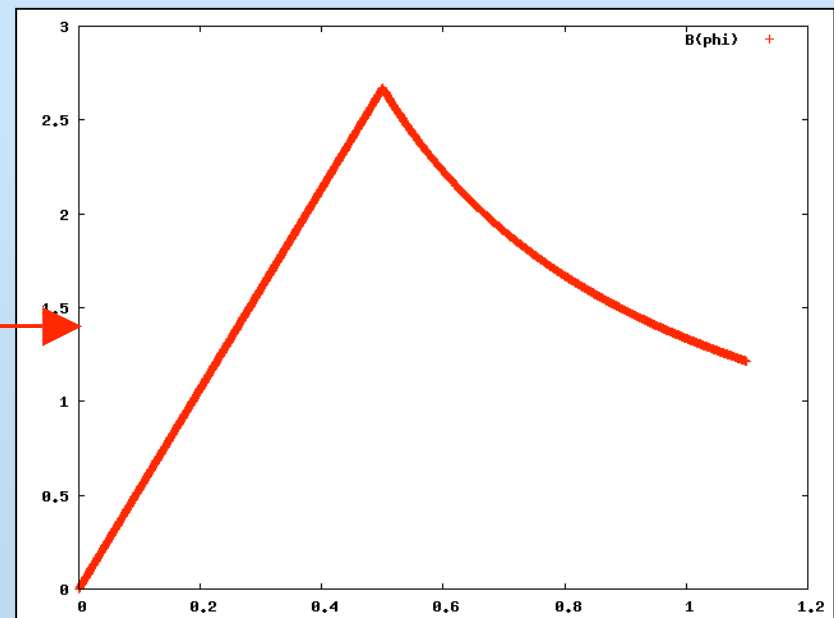
□ $\sigma =$ Magnetization $\sigma_{\phi} = \frac{\langle B_{\phi}^2 / \gamma^2 \rangle}{2\langle p_g \rangle}$ $\sigma_z = \frac{\langle B_z^2 \rangle}{2\langle p_g \rangle}$

□ Poloidal model: uniform B_z

□ Toroidal model:

$$B_{\phi} = \begin{cases} B_m (r/a) & \text{for } r < a \\ B_m (a/r) & \text{for } r > a \end{cases}$$

□ $\alpha =$ Rotation $v_{\phi}(r) = \alpha \frac{B_{\phi}(r)}{B_m}$



Effects of magnetic fields

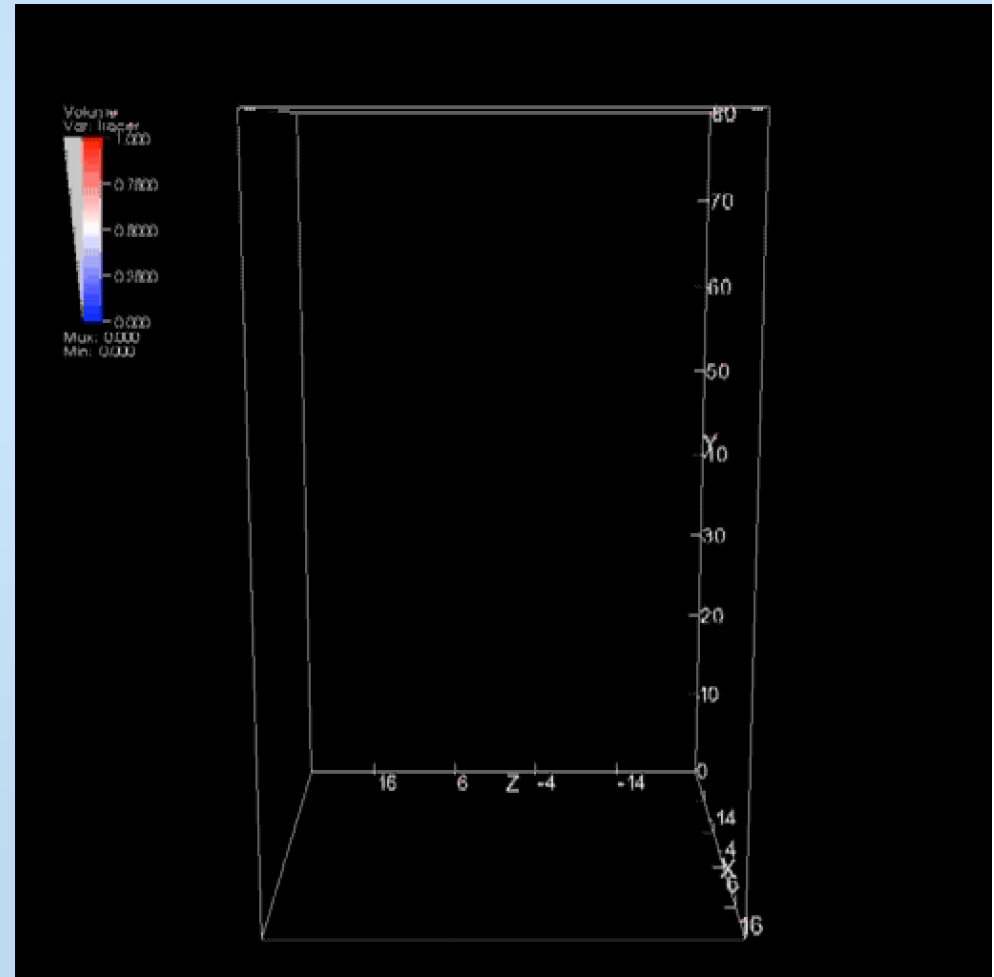
Purely poloidal field:

➤ behaviour similar to the RHD case

$$M_A = \frac{v_j}{v_A} = 1.67 \rightarrow B \approx 10^{-4} G$$

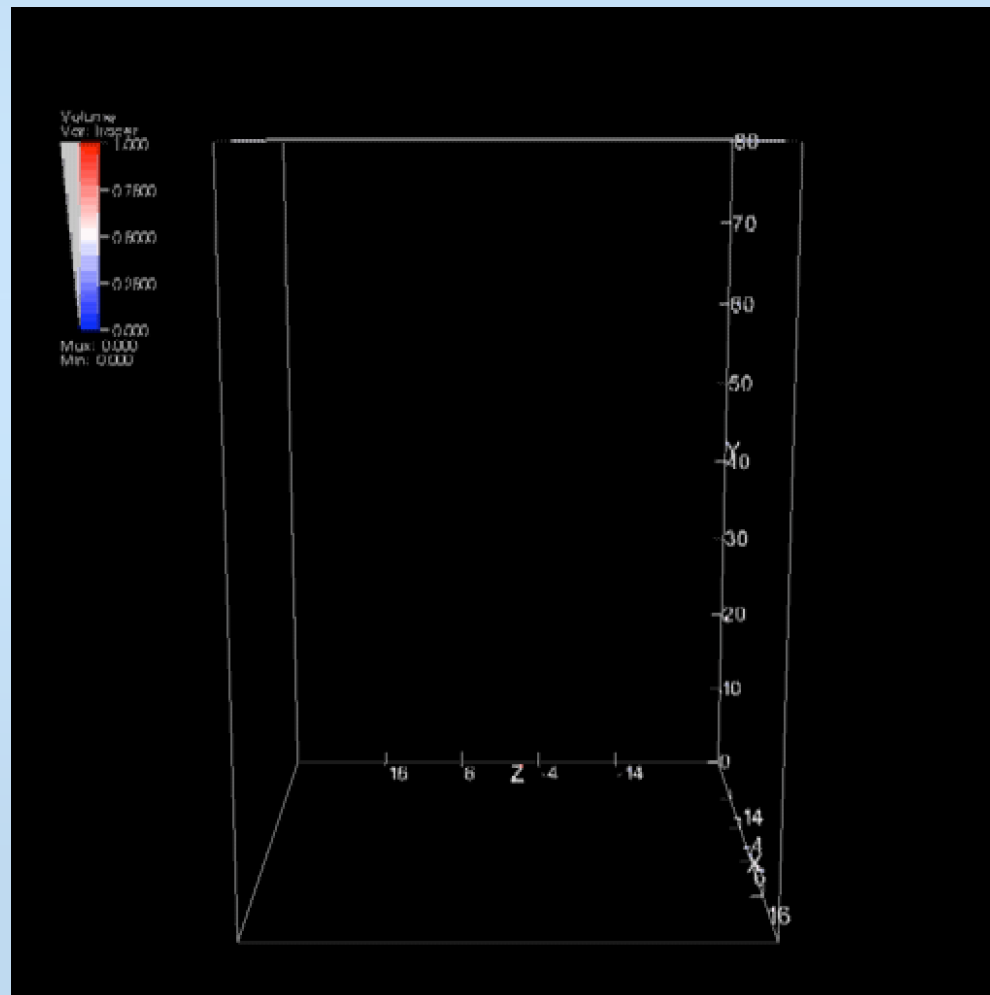
Domain 56x80x56 r_j

Grid 640x1600x640

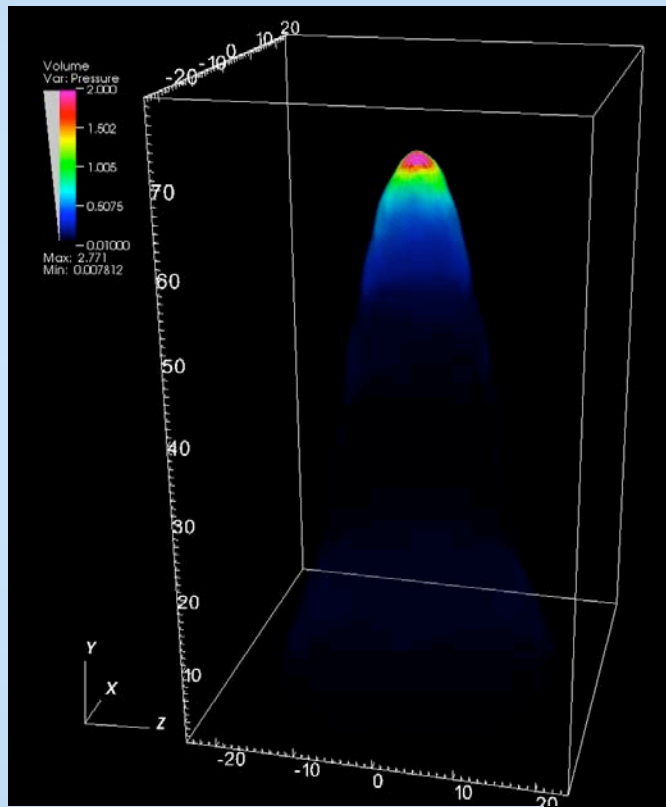


Purely toroidal field:

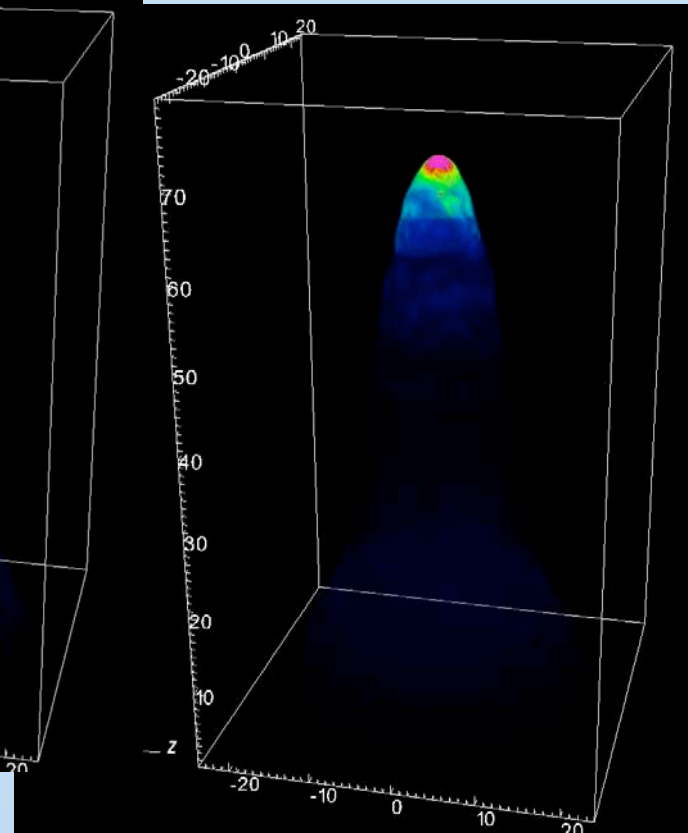
- kink instability induced wiggling
- shielding of the jet inner core, reducing the jet entrainment and braking



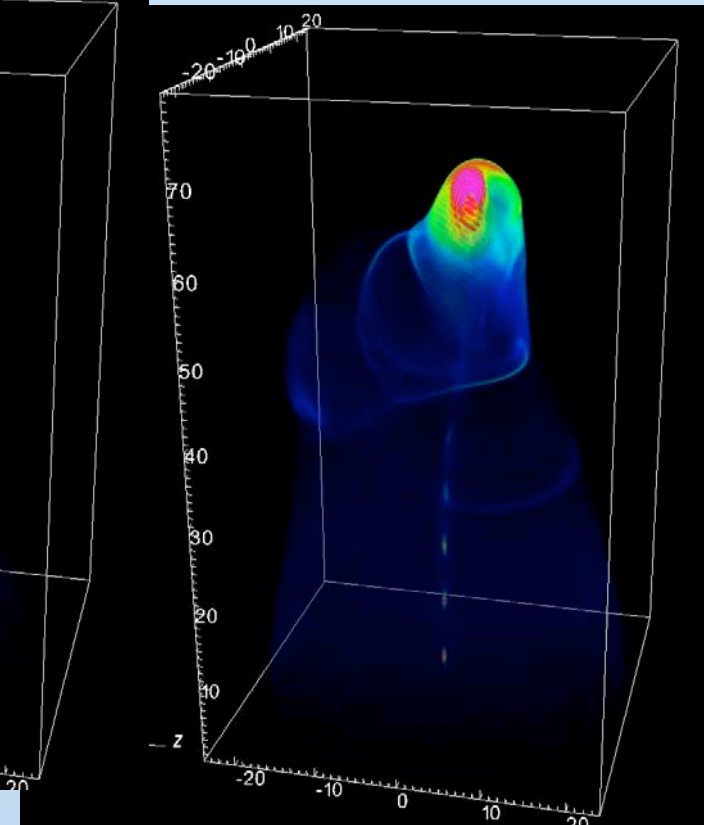
Pressure distribution



RHD
(Hydro)

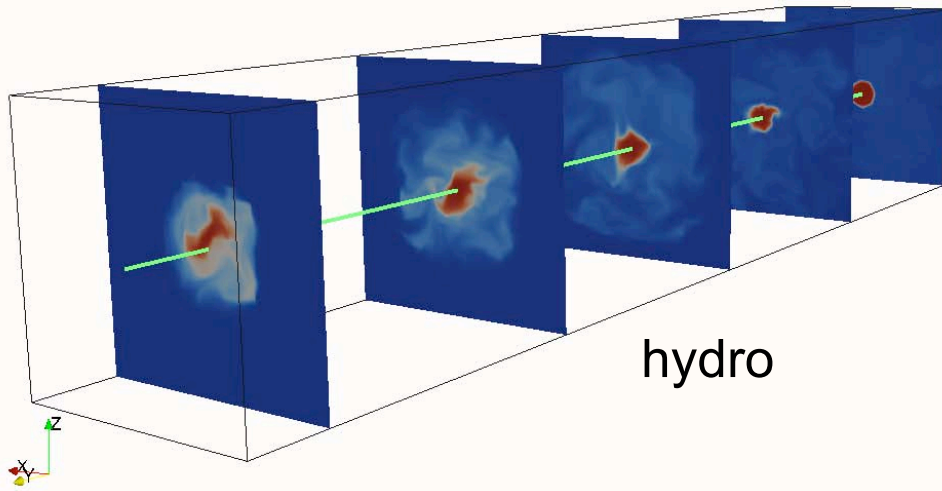


RMHD
Poloidal

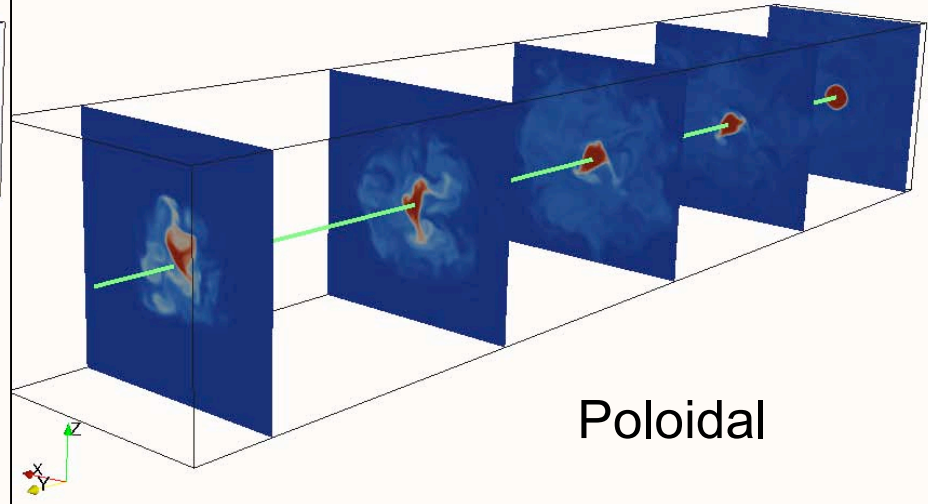


RMHD
Toroidal

Perturbation modes



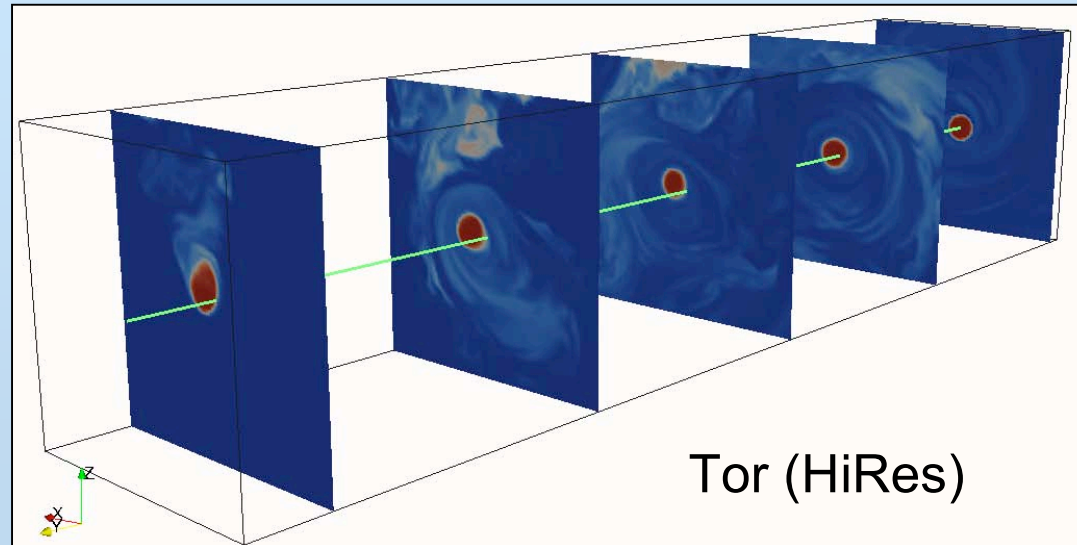
hydro



Poloidal

❑ Hydro case and poloidal case: prevailing of short KH wavelength modes (Massaglia et al. '96, Hardee '87)

❑ Toroidal case show suppression of surface modes, kink modes prevail



Tor (HiRes)

Nonlinear kink instability

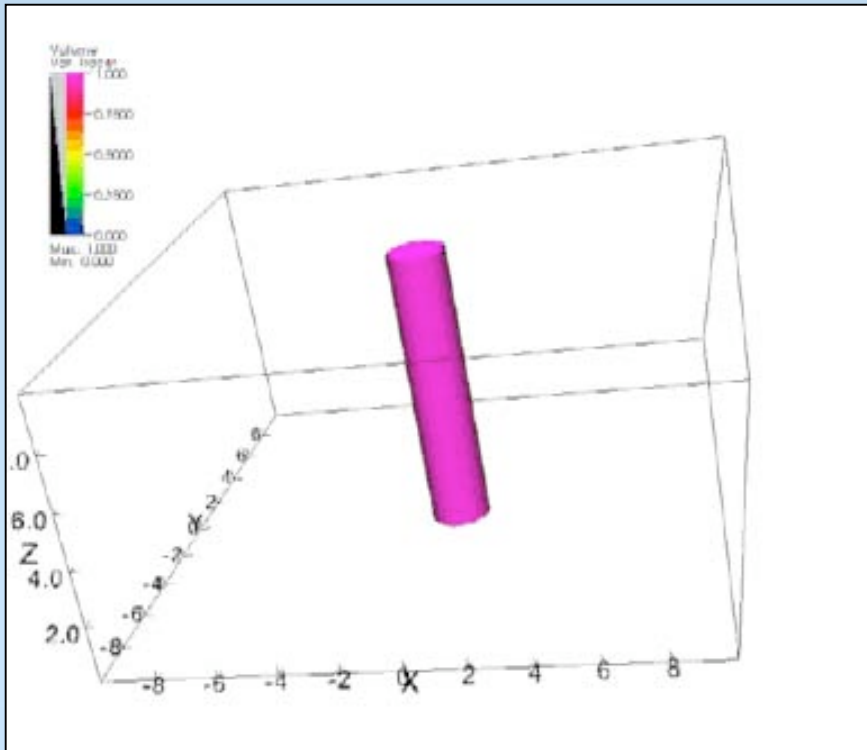
- Assume at equilibrium:
 - $P(r)$ and $\rho(r) = \text{constant}$
 - $B_z(r) = \text{constant}$
 - $\gamma = \text{constant}$ in $r = 0 \div 1$, null elsewhere
 - profile of v_ϕ

$$v_\phi = v_{\phi,M} \frac{r}{b} \left\{ 1 - \exp\left[-(r-1)^3 / a^3 \right] \right\}$$

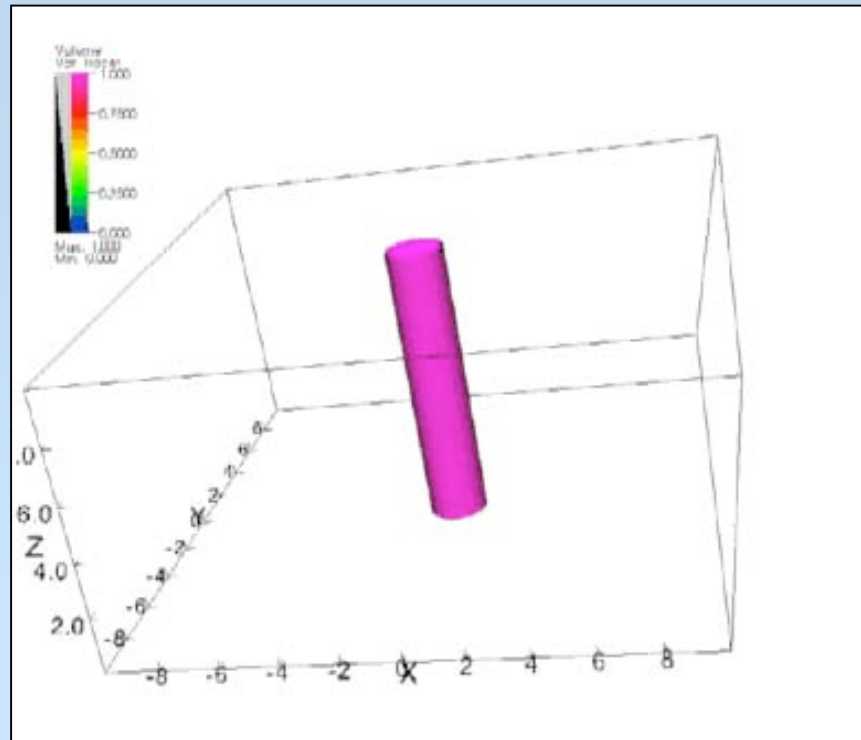
- value of $q = B_\phi / B_z$ where v_ϕ maximum $r \approx 1/2$
 - derive B_ϕ consistently
- Equilibrium equation

$$\frac{w\gamma^2 v_\phi^2}{r} = \frac{1}{r^2} \frac{d}{dr} \left[\frac{(rB_\phi)^2}{2} - \frac{(rE_r)^2}{2} \right]$$

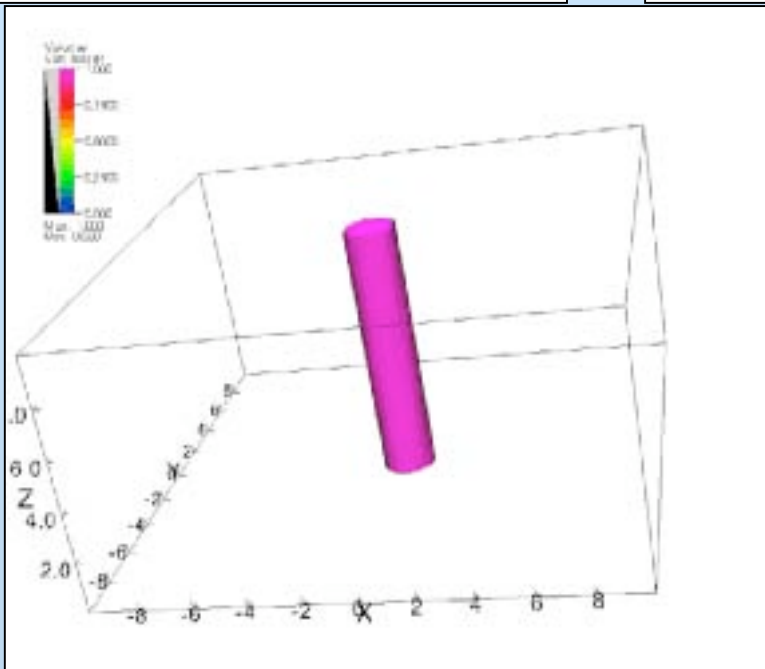
$$E_r = -(v_z B_\phi - v_\phi B_z)$$



g2M1q4

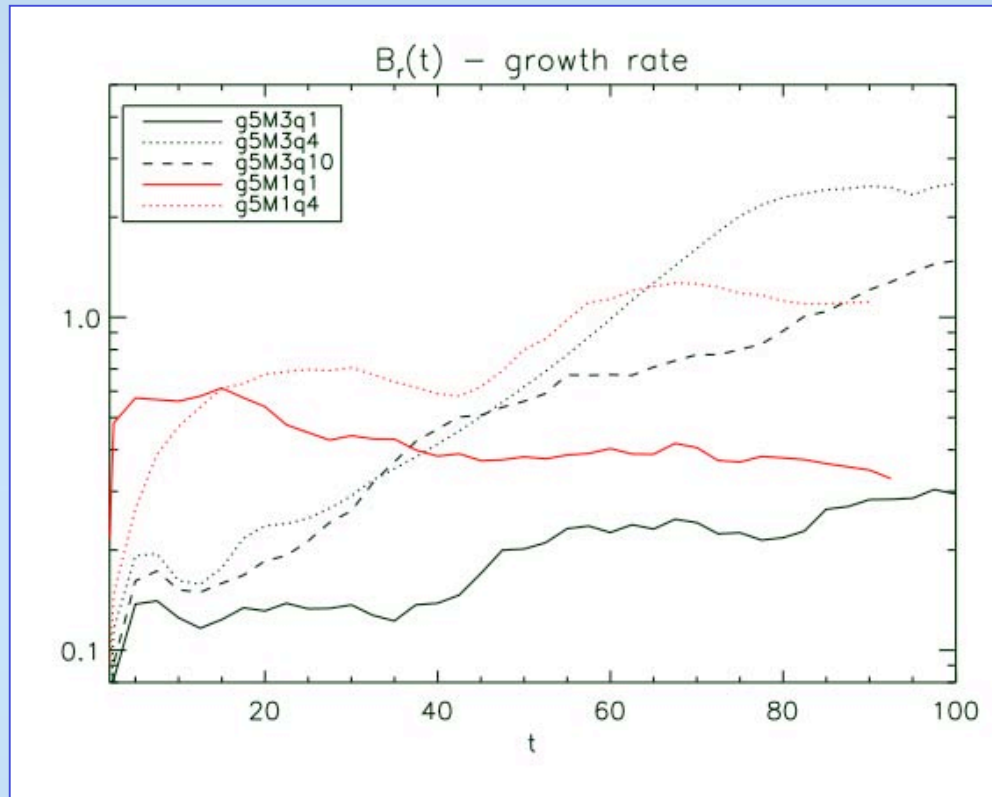


g5M3q4



g5M3q1

- Parametrize solutions with γ , $M_A = w\gamma v^2 / \langle B^2 \rangle$ and q



	γ	M_A	q	stability
g5M3q1	5	3	1	stable
g5M3q4	5	3	4	unstable
g5M3q10	5	3	10	unstable
g5M1q1	5	1	1	stable
g5M1q4	5	1	4	stable
g2M1q4	2	1	4	unstable

- Instability is strong in the non relativistic or weakly relativistic cases for any M_A and $q > 1$
- Instability weaker increasing the magnetic field (decreasing M_A), but likely to reappear for large q (large azimuthal field)
- Instability disappears when the magnetic field is strong enough to move the system towards the force-free field solution, no effect of plasma inertia (Istomin & Pariev)

Kinetic to Poynting flux ratio

- Initial radial equilibrium structure:

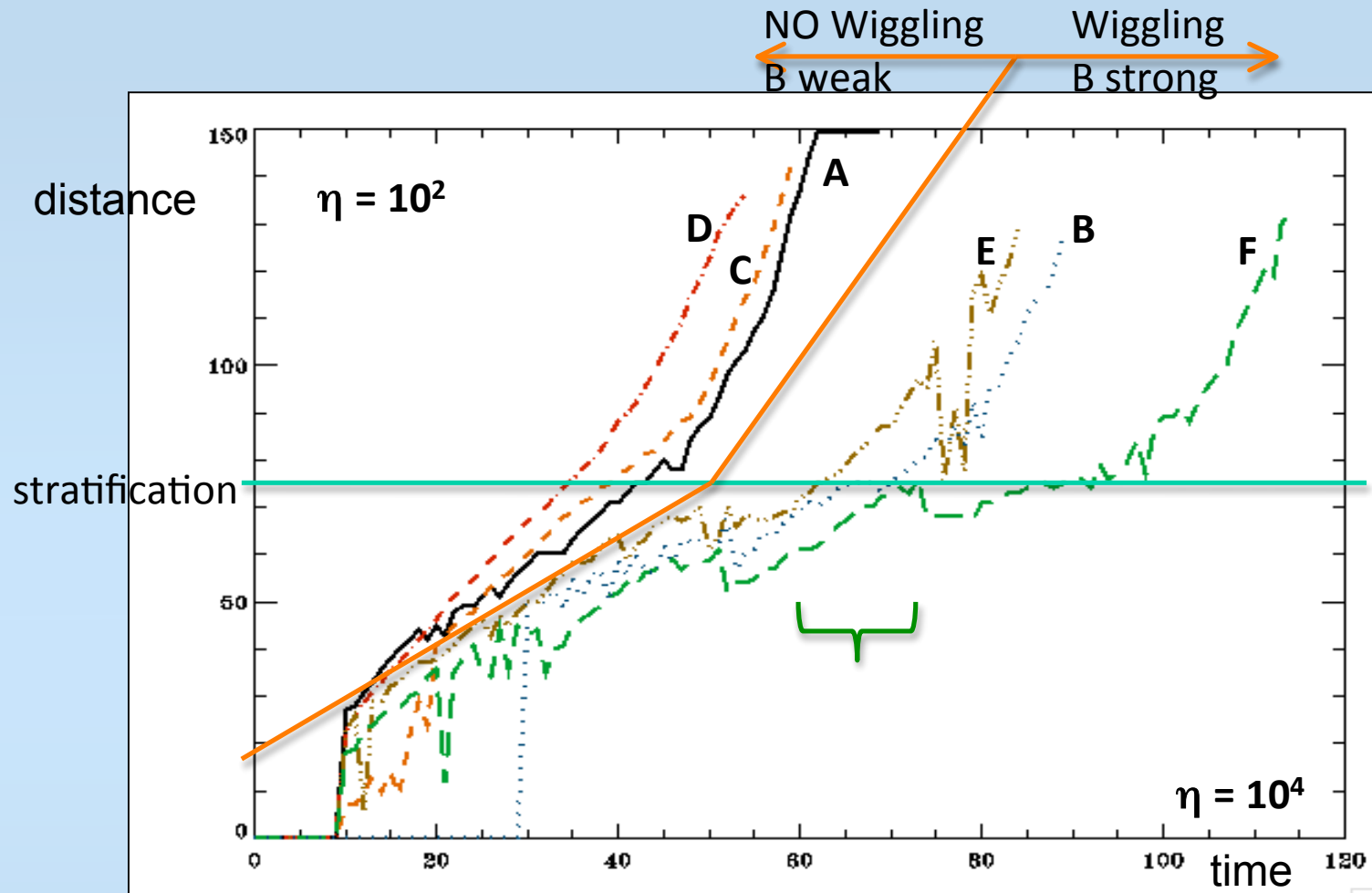
$$\frac{dp}{dr} - \frac{w\gamma^2 v_\phi^2}{r} = (\nabla \cdot \mathbf{E})\mathbf{E} + \mathbf{J} \times \mathbf{B}$$

$$E_r = -(\mathbf{v} \times \mathbf{B})_r = -(v_z B_\phi - v_\phi B_z)$$

$$(\mathbf{J} \times \mathbf{B})_r = -\left[B_z \frac{dB_z}{dr} + \frac{B_\phi}{r} \frac{d}{dr}(rB_\phi) \right]$$

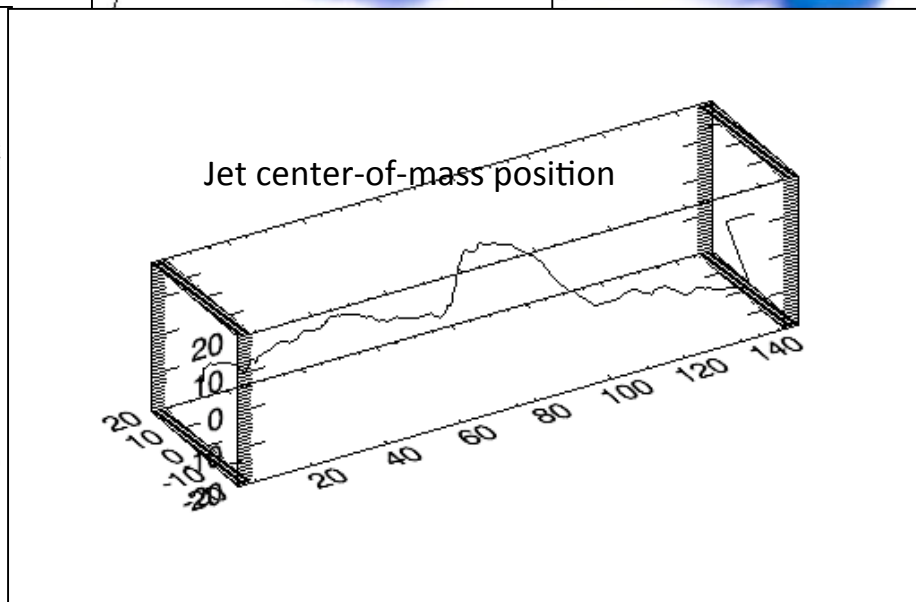
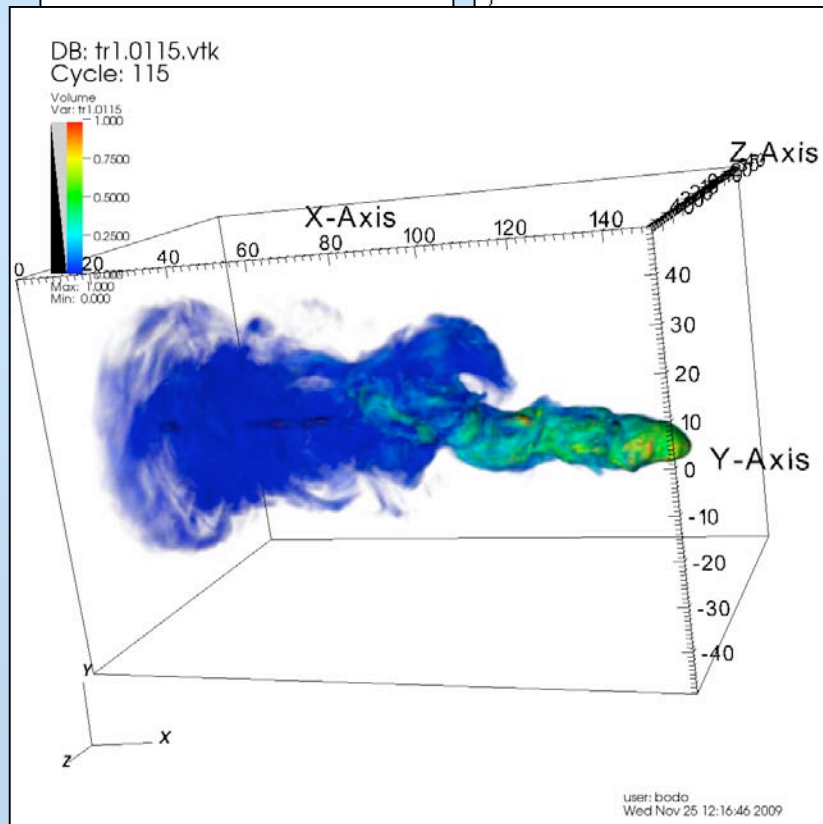
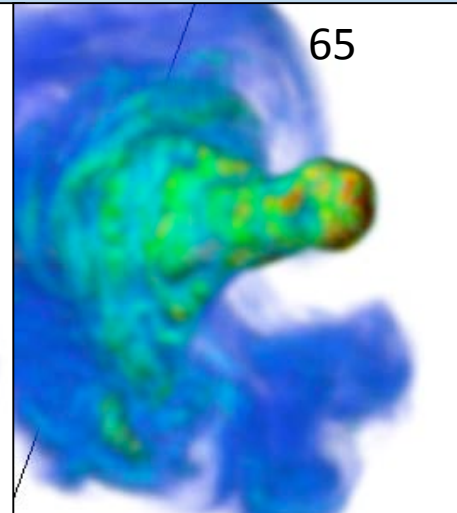
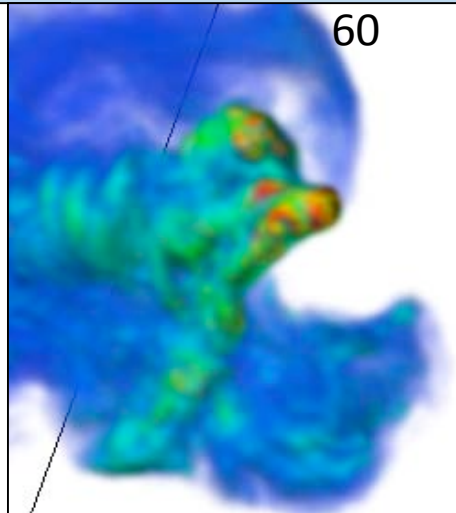
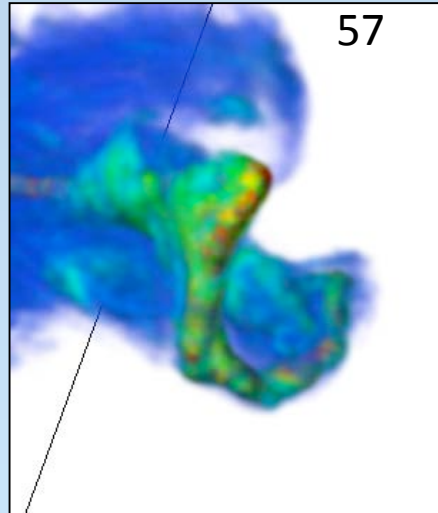
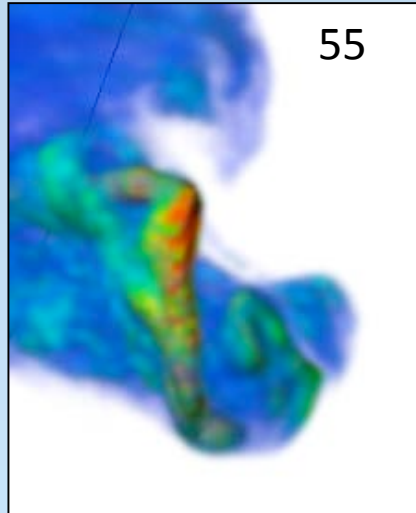
$$-\frac{dp}{dr} + \frac{w\gamma^2 v_\phi^2}{r} = \frac{1}{r^2} \frac{d}{dr} \left[\frac{(rB_\phi)^2}{2} - \frac{(rE_r)^2}{2} \right] + \frac{1}{2} \frac{dB_z^2}{dr}$$

- Relativistic jets at the inlet $\gamma = 10$
- Stratification $\eta = \rho_{\text{amb}}/\rho_{\text{jet}} = 10^4 \rightarrow 10^2$



Fluxes	A	B	C	D*	E	F
F_k/F_P	3.5	1	70	1000	3.5	1
Rotation	0	0	0	0	1	1

*Poloidal field



CASE F

- Large Poynting fluxes produce strong kinks, the head of the flow becomes contorted
- Large kinetic fluxes avoid kinks, the heads of the jet proceeds at large velocity
- The spine of the jet is always highly relativistic on the average, shocks create intermittent structures
- When the jet encounters the low density region its structure becomes again straight and kinks disappear: hints of outflow acceleration ?

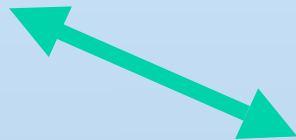
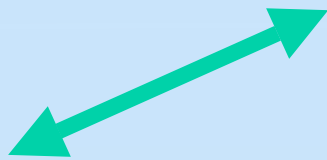


Highly nonlinear (relativistic) physics
Huge extension of physical parameters
Scalability ?

Numerical plasma physics

Astrophysics
Observations

Laboratory plasma physics
Experiments and validation





piston loc



ann
pist

Conclusions

- Relativistic jets show a nonlinear evolution that is different from non relativistic jets in many aspects (AGN vs star)
- Acceleration of relativistic jets in the magneto-centrifugal scheme extends beyond the fast-alfvenic point and is strictly correlated with the collimation process
- Relativistic hydro jets are subject to strong mass entrainment by shear instabilities and form naturally the spine/sheath layer structure
- Relativistic magnetized jets with strong toroidal component are subject to kink instability that may disappear when they emerge from the denser regions
- Entrainment and instabilities do not slow down the spine of the jet that remains relativistic up to the hot spot/termination shock
- The issue of jet acceleration/deceleration requires further analysis of dissipation and turbulent processes
- Particle acceleration: beyond MHD, PIC simulations
- Validation of codes on laboratory experiments is fundamental